

1 **Inference of chromosomal inversion dynamics from**
2 **Pool-Seq data in natural and laboratory populations of**
3 ***Drosophila melanogaster***

4

5 Martin Kapun^{1*}, Hester van Schalkwyk¹, Bryant McAllister², Thomas Flatt^{1*} and Christian
6 Schlötterer^{1#}

7

8 ¹*Institut für Populationsgenetik, Vetmeduni Vienna, Veterinärplatz 1, A-1210 Vienna, Austria*

9

10 ^{*}*Present address: Department of Ecology and Evolution, University of Lausanne, Biophore,*
11 *UNIL Sorge, CH-1015 Lausanne, Switzerland*

12

13 ²*Department of Biology, University of Iowa, Iowa City, Iowa 52242, USA*

14

15 [#]*Corresponding author: Telephone: +43-1-25077-4300; Fax: +43-1-25077-4390; E-mail:*
16 *christian.schloetterer@vetmeduni.ac.at*

17

18 Running title: Inversion frequencies in *Drosophila melanogaster* from Pool-Seq data

19

20 Key words: genomics, inversions, population genetics, Pool-Seq, experimental evolution

21

22

23

24

25 **Article summary**

26 Given their ability to suppress recombination, chromosomal inversions may be key
27 factors shaping genetic variation. Therefore, they have been targeted by numerous
28 studies and particularly regained attention since the advent of next generation
29 sequencing. Here, we present a novel method to estimate inversion frequencies in
30 Pool-Seq data of *D. melanogaster* based on inversion specific marker SNPs. We
31 successfully applied this method to experimental evolution data and detected patterns
32 consistent with positive selection. Moreover, we analyzed clinal frequency patterns
33 along latitudinal gradients and found a previously unknown clinal pattern in a rare
34 cosmopolitan inversion.

35

36

37

38

39

40

41

42

43

44

45

46

47

48

49

50 **Abstract**

51 **Sequencing of pools of individuals (Pool-Seq) represents a reliable and cost-**
52 **effective approach for estimating genome-wide SNP and transposable element**
53 **insertion frequencies. However, Pool-Seq does not provide direct information on**
54 **haplotypes so that for example obtaining inversion frequencies has not been**
55 **possible until now. Here, we have developed a new set of diagnostic marker SNPs**
56 **for 7 cosmopolitan inversions in *Drosophila melanogaster* that can be used to**
57 **infer inversion frequencies from Pool-Seq data. We applied our novel marker set**
58 **to Pool-Seq data from an experimental evolution study and from North**
59 **American and Australian latitudinal clines. In the experimental evolution data,**
60 **we find evidence that positive selection has driven the frequencies of *In(3R)C* and**
61 ***In(3R)Mo* to increase over time. In the clinal data, we confirm the existence of**
62 **frequency clines for *In(2L)t*, *In(3L)P* and *In(3R)Payne* in both North America**
63 **and Australia and detect a previously unknown latitudinal cline for *In(3R)Mo* in**
64 **North America. The inversion markers developed here provide a versatile and**
65 **robust tool for characterizing inversion frequencies and their dynamics in Pool-**
66 **Seq data from diverse *D. melanogaster* populations.**

67

68

69

70

71

72

73

74 **Introduction**

75 Inversions are common chromosomal variants in many organisms; they arise from
76 structural mutations, which cause a complete reversal of linkage among genes relative
77 to the standard chromosomal arrangement. Due to early efforts by Dobzhansky and
78 his coworkers, much of our current understanding of the genetics and evolution of
79 inversion polymorphisms comes from work on species of the genus *Drosophila*
80 (Dobzhansky 1971; Powell 1997). Inversion polymorphisms are pervasive within
81 numerous *Drosophila* species, and a large body of classical work suggests that they
82 are important drivers of evolutionary dynamics and adaptive change in natural
83 populations (for a review see Krimbas and Powell 1992).

84 Several lines of evidence indicate that selection plays a key role in maintaining
85 inversion polymorphisms and in shaping their frequencies in natural populations.
86 First, the frequencies of specific inversion polymorphisms in *Drosophila* have been
87 correlated with numerous life history, physiological, and morphological traits (for
88 reviews see Hoffmann *et al.* 2004, Hoffmann and Rieseberg 2008). Second, numerous
89 polymorphic inversions show strongly clinal (e.g., latitudinal) patterns of variation,
90 and many of these patterns are replicated across continents in broadly distributed
91 species, including, *D. subobscura* (Prevosti *et al.* 1985; Prevosti *et al.* 1988; Krimbas
92 and Powell 1992) *D. melanogaster* (Mettler *et al.* 1977; Knibb *et al.* 1981; Knibb
93 1982), and *D. pseudoobscura* (Dobzhansky and Epling 1944; Dobzhansky 1971;
94 Powell 1997). Third, analyses of latitudinal gradients repeated over time indicate that
95 many of these clines remain stable (Anderson *et al.* 1987) or that they shift with
96 latitude over many years (Anderson *et al.* 2005; Levitan and Etges 2005). Finally, the
97 fitness advantage and the dynamics of inversion heterokaryotypes have been
98 monitored both in natural populations and under laboratory conditions, and the results

99 are often consistent with selection shaping inversion dynamics (Wright and
100 Dobzhansky 1946; Dobzhansky 1971). Moreover, inversions effectively suppress
101 recombination around inverted regions in heterokaryotypes (Sturtevant 1917).
102 Although double cross-overs and gene conversion can maintain a limited amount of
103 gene flux between inverted and non-inverted arrangements (Chovnick 1973; Schaeffer
104 and Anderson 2005), inversions typically cause a pattern of cryptic, chromosome-
105 specific population substructure (Navarro *et al.* 2000). However, despite the large
106 body of work on the population genetics of inversion polymorphisms, the nature of
107 variation harbored by inversions and the molecular targets of selection within
108 inversions remain very poorly understood to date (Hoffmann and Rieseberg 2008).

109 The recent advent of next-generation sequencing technology has revitalized
110 interest in the population genetics of inversion polymorphisms. Several recent studies
111 have used individual-based sequencing across multiple individuals to analyze the
112 details of inversion breakpoint structure, the age of inversions, and patterns of genetic
113 variation associated with inversions in natural populations (Corbett-Detig and Hartl
114 2012; Corbett-Detig *et al.* 2012; Langley *et al.* 2012). However, due to the still
115 relatively high costs associated with sequencing many individuals, the availability of
116 whole-genome population data for multiple individuals remains limited today. A
117 widely used, very simple and cost-effective alternative is to sequence pools of DNA
118 from multiple individuals ("Pool-Seq"; Futschik and Schlötterer 2010), but an obvious
119 drawback of this approach is that it does not yield haplotype information and thus
120 precludes the direct estimation of inversion frequencies.

121 Given the widespread use of the Pool-Seq method in molecular population
122 genomics, and given the importance of inversions in shaping patterns of molecular
123 variation in natural populations, here we have developed a novel set of SNP markers

124 for 7 cosmopolitan inversions in *Drosophila melanogaster* (i.e. *In(2L)t*, *In(2R)Ns*,
125 *In(3L)P*, *In(3R)C*, *In(3R)K*, *In(3R)Mo*, *In(3R)P*). By applying this new marker set to
126 several natural and experimental populations we demonstrate that inversion
127 frequencies and their dynamics can be reliably estimated from and examined with
128 Pool-Seq data.

129

130 **Materials and Methods**

131 We first developed a set of inversion-specific marker SNPs by karyotyping and
132 whole-genome sequencing of individuals from an ongoing experimental evolution
133 study in our laboratory (see Orozoco-terWengel *et al.* 2012; R. Tobler, V. Nolte, J.
134 Hermisson, C. Schlötterer, unpublished results). To supplement this analysis, we also
135 used haplotype information from the *Drosophila* Population Genomics Project
136 (DPGP, DPGP2) (Langley *et al.*, 2012; Pool *et al.* 2012; <http://www.dpgp.org>; for
137 details see below).

138

139 ***Experimental evolution populations***

140 In brief, we carried out an experimental evolution experiment (“laboratory natural
141 selection”, LNS) using an outbred base population of *D. melanogaster* derived from
142 113 isofemale lines isolated from a wild population from Povoia de Varzim (Northern
143 Portugal) in 2008 (see Orozoco-terWengel *et al.* 2012 for details; Tobler *et al.* ,
144 unpublished results). We exposed 3 replicate populations per treatment to two thermal
145 selection regimes, with temperatures changing every 12 hours between 18°C and
146 28°C (“hot”) and between 10°C and 20°C (“cold”). In both treatments, replicate
147 populations were maintained with discrete generations at a fixed population size of
148 1000 individuals per replicate.

149 ***Karyotyping***

150 To determine the distribution of inversions in the above-mentioned selection
151 experiment we used karyotyping. We randomly chose males of unknown
152 chromosomal karyotype from three different cohorts: (1) isofemale lines, which were
153 initially used to establish the base population of the experimental evolution
154 experiment; (2) three replicate populations from the “cold” treatment at generation 34
155 of selection; and (3) three replicate populations from the “hot” treatment at generation
156 60 of selection. Males were crossed to virgin females of an inversion-free mutant
157 strain (*y[1]; cn[1] bw[1] sp[1]*). In the F1, we prepared polytene chromosome
158 squashes from salivary glands of 3rd instar larvae reared at 18°C using orcein staining
159 following standard protocols (Kennison 2000). Chromosome preparations were
160 analyzed using a Leica DM5500B microscope (Leica, Wetzlar, Germany). We
161 determined chromosomal arms using reference maps in Bridges (1935) and Schaeffer
162 *et al.* (2008); inversion loops in heterokaryons were identified from reference
163 photographs in Ashburner *et al.* (1976). Corpses of some larvae used for chromosome
164 preparations were stored in 96% EtOH for later DNA extraction and sequencing.

165

166 ***Single individual sequencing***

167 Based on information from our karyotyping, we selected 15 corpses of F1 larvae from
168 three replicate populations of the hot and the cold selection regime at generations 60
169 and 34, respectively, for whole-genome sequencing (Supporting Table 1). We
170 prepared individual genomic libraries by extracting DNA from homogenized single
171 larva using the Qiagen DNeasy Blood and Tissue Kit (Qiagen, Hilden, Germany) and
172 sheared DNA with a Covaris S2 device (Covaris Inc., Woburn, MA). To identify
173 residual heterozygosity in the reference strain (*y[1]; cn[1] bw[1] sp[1]*) we sequenced

174 a pool of 10 adult females. Each library was tagged with unique 8-mer DNA labels
175 and pooled prior to preparation of a paired-end genomic library using the Paired-End
176 DNA Sample Preparation Kit (Illumina, San Diego, CA); each library was sequenced
177 on a HiSeq2000 sequencer (Illumina, San Diego, CA) (2 x 100 bp paired-end reads).

178

179 ***Mapping of reads***

180 Raw reads were trimmed to remove low quality bases (minimum base quality: 18)
181 using *PoPoolation* (Kofler *et al.* 2011) and mapped against the *D. melanogaster*
182 reference genome (v.5.18) and *Wolbachia* (NC_002978.6) with *bwa* (v.0.5.7; Li and
183 Durbin 2009) using the following parameters: `-n 0.01` (error rate), `-o 2` (gap opening),
184 `-d12, -e 12` (gap length) and `-l 150` (disabling the seed option). We used the *bwa*
185 module `sampe` to reinstate pair-end information using Smith-Waterman local
186 alignment. Using *samtools* (Li *et al.* 2009), we merged SAM files filtered for proper
187 pairs with a minimum mapping quality of 30 in a mpileup file and used *Repeatmasker*
188 3.2.9 (www.repeatmasker.org) to mask simple repetitive sequence and transposable
189 elements (based on the annotation of the *D. melanogaster* genome v. 5.34). Using
190 *PoPoolation*, we masked all indels (and five nucleotides flanking them on either side)
191 present in at least one population and supported by at least two reads to avoid
192 confounding effects of mis-mapping reads containing indels.

193

194 ***Reconstitution of chromosomal haplotypes***

195 We used custom software tools to reconstruct paternal haplotypes from the sequenced
196 F1 larvae (see above). By contrasting polymorphisms present in the F1 larvae to the
197 reference sequence we inferred paternal alleles at heterozygous sites in F1 hybrids.
198 Polymorphic positions (minimum minor allele frequency >10%) in reads from the

199 reference strain (see above) were excluded. In addition, we used the following criteria
200 to avoid false positive paternal alleles or false negative maternal alleles during
201 haplotype reconstruction: (1) we excluded positions with a minimum coverage <15 to
202 reduce false negatives due to large sampling error; (2) we calculated genome-wide
203 coverage distributions for each F1 hybrid and each chromosomal arm separately and
204 excluded positions with a coverage higher than the 95% percentile of the
205 corresponding chromosomal arm to minimize false positives due to mapping errors
206 and duplications; (3) we only included alleles with a minimum count of 20 across all
207 larvae sequenced; (4) for SNPs with more than two alleles we only considered the two
208 most frequent alleles; (5) we only retained alleles for which the allele counts fell
209 within the limits of a 90% binomial confidence interval based on an expected
210 frequency of 50%. The efficiency of our SNP calling was evaluated using two
211 different methods (see Supporting Information).

212

213 ***Fixed differences associated with inversions***

214 We took advantage of a worldwide sample of haplotypes originating from Africa,
215 Europe and North America with known karyotype (Langley *et al.* 2012; Pool *et al.*
216 2012) and combined them with our haplotype data. In total, we compared 167
217 chromosomes from Africa (DPGP2; 107 individuals), Portugal (present study; 15
218 individuals), France (DPGP2; 8 individuals) and USA (DPGP; 37 individuals
219 [consensus genomes]) with known karyotypes, overall representing 7 different
220 inversions (*In(2L)t*, *In(2R)Ns*, *In(3L)P*, *In(3R)C*, *In(3R)K*, *In(3R)Mo*, *In(3R)P*) plus
221 standard chromosome arrangements (Supporting Table 2). For each inversion type,
222 we searched for fixed differences in the combined dataset between inverted
223 karyotypes and all other arrangements (i.e., standard arrangements and overlapping

224 inversions) on the corresponding chromosome in order to identify inversion-specific
225 SNP markers. We excluded positions where less than 80% of all individuals per
226 arrangement were informative. We tested our method as described in the Supporting
227 Information.

228

229 ***Inversion frequency estimates***

230 We used inversion-specific fixed differences between arrangements as SNP markers
231 to estimate inversion frequencies from Pool-Seq datasets of Fabian *et al.* (2012; North
232 American cline), Kolaczkowski *et al.* (2011; Australian cline), Orozco-terWengel *et*
233 *al.* (2012; experimental evolution experiment, “hot” selection regime) and Tobler *et*
234 *al.* (unpublished results; experimental evolution, “cold” regime). Inversion
235 frequencies were estimated from the average of all marker allele frequencies specific
236 to a particular inversion. To reduce the variance in frequency estimates caused by
237 sampling error we excluded all positions with less than 10-fold coverage for all
238 datasets except for the Australia data, where – given the generally low coverage in
239 this dataset – we chose a minimum coverage threshold of three-fold. We also
240 excluded all positions with coverage larger than the 95% percentile of the genome-
241 wide coverage distribution to avoid errors due to mis-mapping or duplications. To
242 evaluate the statistical significance of inversion frequency differentiation over time in
243 our experimental evolution study, we integrated SNP-wise allele frequency
244 information from three replicate populations in each selection regime across multiple
245 timepoints by performing Cochran-Mantel-Haenzel tests (CMH; Landis *et al.* 1978)
246 for each marker SNP separately and by averaging *P*-values across all tests. Since
247 replicates were not available for the two latitudinal datasets, we performed Fisher’s
248 Exact Tests (FET; Fisher 1922) on inversion frequency differences between the

249 lowest-latitude population and all other populations along each cline (North America,
250 Australia) and combined P -values across all marker SNPs. We also compared
251 inversion frequency estimates obtained from SNP markers to our empirical results
252 from karyotyping as described in the Supporting Information. In addition, we also
253 estimated inversion frequencies from our karyotype data and tested for significant
254 differences in inversion frequency between the “hot” and “cold” selection regimes by
255 using the following fully factorial fixed-effects two-way ANOVA model: $y = I + T +$
256 $I \times T$, where y denotes the inversion frequency, I the inversion type and T the
257 selection regime using JMP (v.10.0.0, SAS Institute Inc., Cary, NC).

258

259 ***Genetic variation within inversions***

260 To estimate genetic variation associated with each chromosomal arrangement we
261 estimated π in 100-kb non-overlapping sliding windows for all chromosomes with the
262 same karyotype. We excluded *In(2R)Ns* and *In(3R)P* from this analysis since both
263 inversions were present in only one F1 larva out of the 15 sequenced individuals. To
264 compare π among arrangements we randomly sub-sampled non-inverted chromosomes
265 to match the number of inverted chromosomes for *In(2L)t* and *In(3L)P*. For the
266 inversions on *3R* (*In(3R)Mo* and *In(3R)C*) we were unable to sub-sample because our
267 dataset only contained three chromosomes with standard arrangement on this
268 chromosomal arm. We therefore used all three individual chromosomes to estimate π
269 and F_{ST} among chromosomal arrangements on *3R*. In addition, based on our estimates
270 of π , we calculated F_{ST} between inverted and standard arrangement haplotypes in 100-
271 kb non-overlapping windows to measure the amount of chromosome-wide
272 differentiation among arrangements.

273

274 ***Linkage disequilibrium within inversions***

275 For each chromosomal arm and arrangement, we estimated linkage disequilibrium
276 (LD) by calculating r^2 (Hill and Robertson 1968). We randomly sampled 5000
277 polymorphic SNPs along each chromosomal arm and visualized chromosome-wide
278 pair-wise r^2 -values using heat maps generated from the 'LDHeatmap' package (Shin
279 *et al.* 2006) in R (R Development Core Team 2009). To quantify the difference in
280 overall LD within non-inverted and inverted chromosomes, we averaged all r^2 -values
281 obtained from within the inverted regions for both standard and inverted haplotypes
282 separately and calculated their ratios. Since r^2 depends strongly on the number of
283 haplotypes, we always matched the number of inverted and standard chromosomes by
284 sub-sampling the more frequent chromosomal arrangement.

285

286 ***Expected inversion frequency change under neutrality***

287 To estimate the degree to which inversion frequency changes observed during
288 experimental evolution may be explained by drift alone, we employed forward
289 simulations using a simple Wright-Fisher model of neutral evolution (Otto and Day
290 2007). For computations, we considered an inversion to represent allele A . Inversion
291 frequencies $p_0(A)$ at the beginning of the experiment were obtained from frequency
292 estimates based on our marker SNP approach. Additionally, we used estimates of the
293 effective population size computed from real data of the laboratory natural selection
294 experiment and performed simulations using a value of 200 for the parameter N
295 (Orozco-terWengel *et al.* 2012). Using 100,000 iterations we simulated all three
296 replicate populations for each temperature regime and using the same number of
297 generations and the inversion frequency from the base population. We computed the

298 empirical p-value by determining the number of simulations in which the polarized
299 frequency change in each of the replicates was larger than in the observed data.

300

301 **Results**

302 *Impact of inversions on genetic variation*

303 In total, we identified six polymorphic cosmopolitan inversions segregating in our
304 experimental evolution experiment: four common inversions (*In(2L)t*, *In(2R)Ns*,
305 *In(3L)P*, *In(3R)Payne*) and two rare cosmopolitan inversions (*In(3R)Mo*, *In(3R)C*)
306 (see Mettler *et al.* 1977; Lemeunier and Aulard 1992). We first aimed to examine the
307 partitioning of genetic variation among inversions and standard chromosomes by
308 performing whole-genome sequencing of 15 out of 275 karyotyped individuals and by
309 reconstructing the paternal haplotypes of these flies (see Materials and Methods;
310 Supporting Table 1). We estimated nucleotide diversity (π) and LD (r^2) for both
311 inverted and non-inverted chromosomes and calculated pairwise F_{ST} to estimate
312 genetic differentiation between arrangements. Since *In(2R)Ns* and *In(3R)P* were only
313 represented by one chromosome in our data, we did not analyze these inversions.

314 *2L*: π was similar between the standard arrangement and *In(2L)t* except for the
315 breakpoint regions, where inverted chromosomes were less variable than the standard
316 arrangement. F_{ST} was markedly higher within the inversion breakpoints as compared
317 to the outside of the inverted region (see Supporting Figure 1a), but did not show
318 distinct peaks at the putative breakpoints. Pairwise r^2 values along *2L* indicated the
319 existence of elevated LD in two regions located within the inversion and at the
320 telomeric end of the chromosomal arm in haplotypes carrying *In(2L)t*. LD within
321 inverted haplotypes was 2.46 times higher within the chromosomal region of the

322 inversion as compared to standard arrangement chromosomes (see Supporting Figure
323 2a).

324 *3L*: In contrast to standard arrangement chromosomes, we found reduced
325 variability (\square) around the proximal breakpoint of *In(3L)P* and in two large regions
326 within the inversion as well as downstream of the distal breakpoints in chromosomes
327 carrying the inverted arrangement. Although F_{ST} was homogenous along the
328 chromosome, we detected an unusual haplotype structure in the *In(3L)P*
329 chromosomes, with very large areas of pronounced LD within the inversion and also
330 extending beyond it (see Supporting Figure 1b and Supporting Figure 2b). Overall,
331 LD within inverted haplotypes was approximately 4.7 times higher than in standard
332 chromosomes.

333 *3R*: We found four chromosomal arrangements on the right arm of the third
334 chromosome segregating in the populations from the selection experiment (standard
335 arrangement, *In(3R)C*, *In(3R)Mo*, *In(3R)Payne*, all of which are known to overlap;
336 Lemeunier and Aulard 1992). In contrast to chromosomes carrying *In(3R)C* and
337 *In(3R)Mo*, the standard arrangement chromosomes did not exhibit any regions of
338 reduced heterozygosity (Figure 1). *In(3R)Mo* karyotypes harbored almost no genetic
339 variation within the inverted region, except for two polymorphic regions with a size
340 of approximately 1 and 2 mb, respectively (see Supporting Information for details).
341 Moreover, 2 mb upstream of the proximal breakpoint the *In(3R)Mo* karyotypes were
342 almost completely genetically invariant. We also observed a large haplotype ranging
343 from more than 6 mb upstream to approximately 1 mb downstream of *In(3R)Mo*. In
344 contrast to *In(3R)Mo*, *In(3R)C* did not show any continuous genomic regions
345 exhibiting highly reduced genetic variation. Nonetheless, genetic variation was locally
346 reduced at the breakpoints of the two overlapping inversions *In(3R)Mo* and

347 *In(3R)Payne*. The strongest reduction, showing almost complete absence of genetic
348 variation, was found in a region of approximately 500 kb close to the distal breakpoint
349 of *In(3R)Mo*. However, apart from locally elevated haplotype structure at the
350 proximal breakpoint of *In(3R)C* and the telomeric part of *3R*, we did not observe
351 elevated levels of LD (see Figure 2B). Pairwise F_{ST} was increased for both inverted
352 karyotypes within the inversions as well as in their proximity. Interestingly, we
353 observed peaks of differentiation only at the proximal breakpoints of both inversions
354 but not at their distal breakpoints. Moreover, despite pronounced haplotype structure
355 in *In(3R)Mo*, we failed to find strong differences in LD between the different
356 arrangements (*In(3R)Mo*, LD ratio: 1.05; *In(3R)C*, LD ratio: 1.13).

357

358 ***Identification of inversion-specific SNPs***

359 Next, we used our data to define inversion-specific SNPs that could be used as
360 diagnostic markers for detecting and surveying specific inversions. Alleles private to
361 *In(2L)t*, *In(3L)P*, *In(3R)K*, and *In(3R)Payne* were almost entirely restricted to the
362 inversion breakpoints (Figure 3). In contrast, alleles specific to *In(2R)Ns* and *In(3R)C*
363 were distributed throughout these inversions (Figure 3). For *In(3R)Mo*, we not only
364 found marker SNPs within the inversion but also a surplus of SNPs beyond the
365 proximal and distal breakpoints (Figure 3). The number of marker SNPs in the
366 different inversions varied greatly, ranging from 4 in *In(3R)K* to 150 in *In(3R)Mo*
367 (Supporting Table 3). Importantly, two complementary methods for detecting false
368 positives and a comparison of inversion frequency estimates based on karyotyping
369 versus marker SNPs indicated that our SNP marker set is highly reliable (Supporting
370 Information).

371

372 ***Inversion dynamics during experimental evolution***

373 We used these inversion-specific marker SNPs to investigate the dynamics of
374 inversions during our experimental evolution experiment, using three replicate
375 populations in each selection regime. For each inversion, we estimated its frequency
376 by averaging over the frequencies of all inversion-specific SNP markers. With a
377 baseline frequency of about 40% in the base population, *In(2L)t* was the most
378 frequent inversion in the experiment. Its frequency fluctuated unpredictably across
379 selection regimes and replicate populations, but the inversion remained polymorphic
380 throughout the experiment with frequencies larger than 20% (see Figure 4, Supporting
381 Figure 3A, Supporting Table 4). In contrast, *In(2R)Ns* started out at a frequency of
382 approximately 10% in the base populations and then consistently decreased in all
383 replicates in both selection regimes (Figure 4, Supporting Figure 3B, Supporting
384 Table 4). This pattern resulted in a statistically significant difference in inversion
385 frequency between the base population and the third time point examined in both
386 thermal selection regimes (Supporting Table 5). Similarly, *In(3R)Payne* decreased
387 significantly in frequency in both regimes (see Figure 4, Supporting Figure 3G,
388 Supporting Table 4), a trend already noticed by Orozco-terWengel *et al.* (2012) for
389 the “hot” regime. Interestingly, three inversions showed a selection regime-specific
390 behavior. While *In(3L)P* remained stable around 15% in the “cold” regime, it
391 decreased significantly over time in the “hot” regime (Figure 4, Supporting Figure
392 3C, Supporting Table 4). In contrast *In(3R)Mo* initially segregated at a very low
393 frequency of approximately 5% in the base populations but then consistently
394 increased to >25% in all replicates of the “cold” regime while showing inconsistent
395 frequency patterns in the “hot” regime (Figure 4, Supporting Figure 3F). Finally,
396 *In(3R)C* started out at approximately 15%, then strongly increased over time in all

397 replicates of the “hot” regime, but fluctuated unpredictably in the “cold” regime
398 (Figure 4, Supporting Figure 3D). In good agreement with these changes in inversion
399 frequencies as estimated from our SNP markers, we found highly significant effects
400 of inversion type (2-way ANOVA, $F_{5,24} = 21.339$, $P < 0.0001$) and of the inversion
401 type by selection regime interaction ($F_{5,24} = 6.9793$, $P < 0.001$) in our data based on
402 inversion frequencies observed from 275 karyotyped larvae, confirming again the
403 reliability of our novel inversion-specific SNP markers.

404

405 *Spatial distribution of inversions in natural populations*

406 We next used our inversion-specific SNPs to estimate inversion frequencies in two
407 previously published Pool-Seq datasets of populations collected along latitudinal
408 clines in North America (Fabian *et al.* 2012) and Australia (Kolaczkowski *et al.*
409 2011). For the North American data we found a clinal distribution of most inversions
410 (Supporting Figure 4A, Supporting Table 6). *In(2L)t*, *In(3L)P* and *In(3R)Payne*
411 showed strongly clinal patterns negatively correlated with latitude (Supporting Table
412 7). While *In(2L)t* and *In(3L)P* decreased linearly from south (Florida) to north
413 (Maine), *In(3R)Payne* was very frequent (~50%) in Florida but almost absent in
414 Pennsylvania and Maine (also see Fabian *et al.* 2012). In contrast, the frequencies of
415 *In(2R)Ns*, *In(3R)K* and *In(3R)Mo* increased with latitude. *In(3R)C* segregated at very
416 low frequencies and showed no clinal pattern.

417 Similarly, we estimated inversion frequencies for the two endpoints of the parallel
418 but independent Australian cline (Queensland and Tasmania; cf. Kolaczkowski *et al.*
419 2011) (Supporting Figure 4B, Supporting Table 6). Similar to the patterns we
420 observed for the North American cline, we found that *In(2L)t*, *In(3L)P* and
421 *In(3R)Payne* were much more frequent at low latitude (Queensland) but absent or at

422 low frequency at high latitude (Tasmania). However, none of the observed frequency
423 differences were significant according to FET (see Supporting Table 7), maybe due to
424 the low sequence coverage in this dataset. We did not detect the presence of *In(2R)Ns*,
425 *In(3R)C*, *In(3R)K* and *In(3R)Mo* in the Australian dataset, but due to low coverage we
426 were unable to determine whether these inversions occur at a very low frequency or
427 whether they are truly absent.

428

429 **Discussion**

430 Numerous previous studies have aimed to understand patterns of genetic variation
431 associated with inversions in *D. melanogaster* (e.g., see Andolfatto *et al.* 2001, and
432 references therein). Fixed genetic differences associated with inversions have been of
433 particular interest since they may provide valuable information about the evolutionary
434 history of these structural variants. For example, variation around inversion
435 breakpoints has frequently been used to estimate inversion age (e.g., Hasson and
436 Eanes 1996; Andolfatto *et al.* 1999; Matzkin *et al.* 2005). However, previous studies
437 have been limited by the restricted amount of available data, and especially by the
438 paucity of reliable molecular markers for detecting and surveying inversions in *D.*
439 *melanogaster*.

440 Here, we have aimed to extend these efforts by using a combination of next-
441 generation whole-genome sequence analysis and classical karyotyping of inversions
442 in *D. melanogaster*. Specifically, by combining haplotype data from our present study
443 (based on both individual-level sequencing and karyotyping) with publicly available
444 haplotype information from known karyotypes in the DPGP and DPGP2 data, we
445 have developed a new and extensive set of inversion-specific marker SNPs. These
446 novel diagnostic markers have allowed us characterize the frequency dynamics of 7

447 polymorphic inversions in both laboratory and natural populations of *D.*
448 *melanogaster*.

449

450 ***Patterns of divergence in chromosomal inversions***

451 Overall, we observed large heterogeneity in the number and distribution of divergent
452 SNPs for different inversions. In three of the common large cosmopolitan inversions
453 (*In(2L)t*, *In(3L)P* and *In(3R)Payne*) and in the rare large cosmopolitan inversion
454 *In(3R)K* we found only few divergent SNPs, most of which were restricted to the
455 inversion breakpoints. These patterns agree well with previous observations for
456 *In(2L)t* and *In(3L)P* (Andolfatto *et al.* 2001) and provide further evidence that
457 suppression of gene flux is mainly restricted to only a few kb around the inversion
458 breakpoints.

459 For *In(2R)Ns*, which is also considered to be common cosmopolitan inversion and
460 which has a similar age as *In(2L)t*, *In(3L)P*, *In(3R)Payne* and *In(3R)K* (Corbett-Detig
461 and Hartl 2012), we identified fixed differences throughout the whole inversion. This
462 inversion is markedly smaller than the other cosmopolitan inversions (~4.8 mb),
463 resulting in an effective recombination rate of approximately 18cM across the
464 inverted region (e.g., Fiston-Lavier *et al.* 2010; Comeron *et al.* 2012). Since double
465 crossing-over is unlikely to occur in regions of less than 20cM (Navarro *et al.* 1997),
466 presumably because the minimum distance between chiasmata is limited by crossing-
467 over interference (McPeck and Speed 1995), the pattern we have observed for
468 *In(2R)Ns* might reflect low rates of gene conversion.

469 Similar to *In(2R)Ns*, we found that for two rare cosmopolitan inversions on 3R
470 (*In(3R)C*, *In(3R)Mo*) fixed differences were also not restricted to the breakpoint
471 regions. *In(3R)C* is a large terminal inversion (> 12mb), and marker SNPs for this

472 inversion showed a pronounced non-homogeneous distribution. SNPs were found
473 across the distal half of the inverted region, perhaps reflecting reduced recombination
474 close to the telomere rather than an inversion-specific pattern. Alternatively, this
475 pattern might reflect selection of co-adapted *In(3R)C*-specific alleles. However, since
476 *In(3R)C* haplotypes were only available from one population from Portugal, we
477 cannot rule out that these patterns are highly specific.

478 The number and distribution of marker SNPs for *In(3R)Mo* differed markedly
479 from all other inversions. For this inversion, we detected the highest number of
480 marker SNPs and found them to be distributed inside the inversion as well as beyond
481 the inversions boundaries, both proximal and distal. This strongly suggests that
482 suppression of recombination occurs well beyond the inversion breakpoints.

483

484 ***Distribution of inversions in natural populations***

485 The pervasive clinal distribution of the cosmopolitan inversions *In(2L)t*, *In(3L)P* and
486 *In(3R)Payne* along latitudinal gradients is well-known and has been documented for
487 numerous populations in North America, Australia, and Asia already over 30 years
488 ago (Knibb 1982). The fact that qualitatively similar frequency clines for these
489 inversions have been observed on multiple continents has been taken as strong *prima*
490 *facie* evidence for the non-neutral maintenance of these inversions by spatially
491 varying selection. However, up-to-date no conclusive data have been published about
492 whether the clinal patterns for these inversions have remained stable or not. While
493 two studies from Australia (Anderson *et al.* 1987; Anderson *et al.* 2005) found that
494 inversion clines remained stable or shifted with latitude, a study from Japan observed
495 pronounced changes in some populations over many years (Inoue *et al.* 1984). We
496 were therefore interested in using our inversion-specific SNP markers to examine

497 inversion frequencies in recently generated Pool-Seq data for the North American
498 (Fabian *et al.* 2012) and Australian (Kolaczowski *et al.* 2011) clines.

499 Despite a large difference in sequence coverage between these two recent studies
500 (approximately 45-fold versus 11-fold coverage), we observed clinal frequency
501 patterns for *In(2L)t*, *In(3L)P* and *In(3R)Payne* that are in excellent qualitative
502 agreement with previous findings from the 1970s and 1980s (Mettler *et al.* 1977;
503 Knibb *et al.* 1981; Knibb 1982) for both the Australian and the North American cline.
504 Remarkably, our data suggest that the inversion frequencies for *In(3R)Payne* and
505 *In(3L)P* have remained extremely stable for more than 30 years. In contrast, for
506 *In(2L)t* we also observed clinal variation but detected an increase in the frequency of
507 this inversion by approximately 20% in all populations as compared to previous
508 observations. Although we observed strong inversion clines in the data from the
509 Australian east coast that are qualitatively consistent with previous studies, our
510 inversion frequency estimates for Australia were generally lower than those reported
511 in previous work. While it is possible that these results reflect a reduction in inversion
512 frequencies in Australia in recent years, we cannot rule out that the low sequencing
513 coverage of the Australian data has downward-biased our estimates. Clearly, further
514 in-depth analysis of these inversions will be necessary to understand the mechanisms
515 that determine their dynamics and maintenance.

516 *In(2R)Ns*, in contrast, showed a different pattern to that observed for *In(2L)t*,
517 *In(3L)P* and *In(3R)Payne*. Two earlier studies found this inversion to occur at a
518 frequency of >20% in Queensland (Mettler *et al.* 1977; Knibb *et al.* 1981), but our
519 analysis of the Australian data suggests that this inversion has either decreased to very
520 low frequencies or that it has completely vanished in Australia. For the North
521 American cline we also found a pattern that contrasts with previous results: Mettler *et*

522 *al.* (1977) reported that the frequency of *In(2R)Ns* decreases with increasing latitude,
523 whereas in our analysis this inversion showed a weakly (non-significant) clinal trend
524 from approximately 0-1% frequency in Florida up to 7-10% in Maine.

525 The three rare cosmopolitan inversions *In(3R)C*, *In(3R)K* and *In(3R)Mo* were
526 either not present in the Australian data or segregated at frequencies below our
527 detection threshold. In contrast, for the North American east coast, we found both
528 *In(3R)C* and *In(3R)K* to be segregating at very low frequencies, consistent with
529 previous observations (Mettler *et al.* 1977; Knibb 1982). Surprisingly, while
530 *In(3R)Mo* was found to be very rare and non-clinal in North America 30 years ago
531 (e.g., Mettler *et al.* 1977) we now detect a positive correlation with latitude. This is
532 consistent with the data of Langley *et al.* (2012) who have recently noticed a
533 considerable increase in *In(3R)Mo* frequency (up to a frequency of approximately
534 18% in Raleigh, North Carolina). Together, our data indicate that *In(3R)Mo* has
535 recently undergone a strong increase in frequency along the North American east
536 coast. Although the reasons for this striking pattern remain unclear, the strong
537 reduction of genetic variation within and around *In(3R)Mo* described here and in two
538 other recent studies (Langley *et al.* 2012; Corbett-Detig and Hartl 2012) is consistent
539 with this notion and indicates a recent origin coupled with a rapid increase in
540 frequency.

541

542 ***Implications of inversion polymorphisms for genome scans of selection***

543 Our investigation of inversion frequency dynamics during experimental evolution
544 clearly demonstrates that the frequencies of some inversions change consistently
545 among replicate populations. While some inversions decreased in frequency in both
546 thermal selection regimes, three of them changed consistently in frequency in only

547 one of the selection regimes. A meta-analysis of inversion frequency changes during
548 experimental evolution by Inoue (1979) has reported that inversion frequencies
549 generally decrease during experimental evolution. However, in contrast to Inoue
550 (1979), we found two inversions (*In(3R)C* and *In(3R)Mo*) whose frequencies clearly
551 and consistently increased over time in one of the selection regimes in our
552 experimental evolution study. Wright-Fisher simulations of neutral evolution based
553 on the initial inversion frequencies show that frequency changes observed for these
554 two inversions were significantly higher than expected due to genetic drift alone (see
555 Supporting Table 8). Thus, this pattern strongly suggests that both inversions must
556 likely have carried one or several selection regime-specific favorable alleles.
557 Interestingly, and perhaps consistent with a selective role for this inversion, *In(3R)C*
558 has previously been shown to affect bristle number variation in an artificial selection
559 experiment (Izquierdo *et al.* 1991), yet we did not monitor this phenotype in our
560 experimental evolution study.

561 In a genome-wide analysis of our “hot” selection regime, Orozco-terWengel *et al.*
562 (2012) have identified the majority of candidate SNPs to be located on chromosome
563 *3R*, which also harbors four overlapping inversions. Strikingly, two of these
564 inversions, *In(3R)C* and *In(3R)Payne*, changed significantly in frequency in the “hot”
565 regime over the experiment, perhaps suggesting that beneficial alleles in these
566 inversions have been major targets of selection. Yet, among the most significant
567 candidate SNPs identified by Orozco-terWengel *et al.* (2012) only 1-3 of the marker
568 SNPs for *In(3R)C* (depending on the dataset analyzed) overlapped the candidate SNPs
569 sets. If the inversion was the only cause for the strong molecular signature of selection
570 on *3R* in this experiment, these inversion-specific SNPs would clearly be expected to
571 show the largest allele frequency differences, yet they do not. Instead, we hypothesize

572 that the presence of inversions in laboratory populations can result in cryptic
573 chromosome-specific population structure which in turn causes elevated drift and
574 leads to a surplus of candidate SNPs. If selection is assumed to operate on top of this
575 structure, the interpretation of the SNP data becomes very challenging. Thus, even
576 though the inversions might play an important role in the response to selection,
577 distinguishing the effects due to selection from those due to population structure is
578 practically difficult. One way around this problem in experimental evolution studies
579 using *Drosophila* would be to use inversion-free *Drosophila* species.

580 In natural populations we have observed a similar phenomenon. Despite almost all
581 sites being shared between *In(3R)Payne* and the non-inverted chromosome,
582 populations with a high *In(3R)Payne* frequency seem to harbor more variation (also
583 see Fabian *et al.* 2012), as might be expected for a subdivided population. Since
584 inverted and non-inverted chromosomes will have different allele frequencies, the
585 contrast of populations with different inversion frequencies for the inference of
586 selection is also challenging. On the other hand, in our previous study of clinal
587 variation along North American cline, we found 77% of all clinal candidate SNPs to
588 be located on *3R* and >50% of the candidates within the region spanned by
589 *In(3R)Payne*, a highly non-random pattern that is consistent with spatially varying
590 selection (Fabian *et al.* 2012) and that is also qualitatively mirrored in the Australian
591 data (Kolaczowski *et al.* 2011). Nonetheless, due to the difficulty of teasing apart the
592 effects of demography and population structure versus those of selection, we
593 anticipate that in the future genome scans of selection might preferentially focus on
594 chromosomes with the same inversion status or use inversion-free systems.

595

596

597 **Conclusions**

598 Here we have presented a novel and robust set of molecular SNP markers for seven
599 polymorphic chromosomal inversions in *D. melanogaster*, which will be highly useful
600 for the analysis of Pool-Seq data in this model. Although overall we have found a
601 good correlation between our SNP-based and karyotype-based inversion frequency
602 estimates, we would like to caution that our inference of inversion-specific SNPs is
603 highly dependent on the available reference genomes. In particular, for *In(3R)C*,
604 *In(3R)K* and *In(3R)Mo*, which did not occur in all populations in our combined
605 dataset, we cannot rule out that our marker SNP sets contain some false positives.
606 Therefore, for diverged populations, inversion frequency estimates may be less
607 accurate. Yet, given that multiple SNPs contribute to the estimates of inversion
608 frequencies, we expect that our set of inversion-specific markers will show a reliable
609 performance across all *Drosophila* populations.

610

611 **Data accessibility**

612 The raw FASTQ files for all single individuals are available from the European
613 Sequence Read Archive (http://www.ebi.ac.uk/ena/about/search_and_browse) under
614 the accession number XXX.

615 Reconstructed haploid genomes (available as FASTA files) as well as a collection
616 of custom written Python scripts are available from the Dryad database
617 (<http://datadryad.org>) under the accession: XXX

618

619

620

621

622 **Acknowledgements**

623 We thank all the members of the Institute of Population Genetics for their support, in
624 particular Andrea Betancourt for helpful discussion, Raymond Tobler for sharing
625 unpublished data, and Daria Martynow, Daniel Fabian and Raymond Tobler for help
626 with karyotyping. Above all, we are grateful to Viola Nolte for library construction
627 and handling the sequencing data. Our work was supported by the Austrian Science
628 Foundation (FWF P19467 grant to CS) and the Swiss National Science Foundation
629 (SNF PP00P3_133641 grant to TF). BFM was supported by a Fulbright grant from
630 the Austrian-American Educational Commission.

631

632 **References**

- 633 Anderson A. R., Hoffmann A. A., McKechnie S. W., Umina P. A. and A. R. Weeks,
634 2005 The latitudinal cline in the *In(3R)Payne* inversion polymorphism has shifted
635 in the last 20 years in Australian *Drosophila melanogaster* populations. *Molecular*
636 *Ecology* **14**: 851–858.
- 637 Anderson P. R., Knibb W. R. and J. G. Oakeshott, 1987 Inversion polymorphisms and
638 nucleotide variability in *Drosophila*. *Genetical Research* **77**: 1–8.
- 639 Andolfatto P., Wall J. D. and M. Kreitman, 1999 Unusual haplotype structure at the
640 proximal breakpoint of *In(2L)t* in a natural population of *Drosophila*
641 *melanogaster*. *Genetics* **153**: 1297–1311.
- 642 Andolfatto P., Depaulis F. and A. Navarro, 2001 Inversion polymorphisms and
643 nucleotide variability in *Drosophila*. *Genetical Research* **77**: 1–8.
- 644 Ashburner M. and F. Lemeunier, 1976 Relationships within the *melanogaster* species
645 subgroup of the genus *Drosophila* (*Sophophora*) i. inversion polymorphisms in
646 *Drosophila melanogaster* and *Drosophila simulans*. *Proc R Soc Lond, B, Biol Sci*

647 **193**: 137–157.

648 Bridges C., 1935 Salivary chromosome maps. *J Hered* **26**: 60–64.

649 Chovnick A., 1973 Gene conversion and transfer of genetic information within the
650 inverted region of inversion heterozygotes. *Genetics* **75**: 123–131.

651 Comeron J. M., Ratnappan R. and S. Bailin, 2012 The many landscapes of
652 recombination in *Drosophila melanogaster*. *PLoS Genet* **8**: e1002905.

653 Corbett-Detig R. B. and D. L. Hartl, 2012 Population Genomics of Inversion
654 Polymorphisms in *Drosophila melanogaster*. *PLoS Genet* **8**: e1003056.

655 Corbett-Detig R. B., Cardeno C. and C. H. Langley, 2012 Sequence-based detection
656 and breakpoint assembly of polymorphic inversions. *Genetics* **192**: 131–137.

657 Dobzhansky T. G. and C. Epling, 1944 *Contributions to the genetics, taxonomy, and*
658 *ecology of Drosophila pseudoobscura and its relatives*. Carnegie Institution of
659 Washington.

660 Dobzhansky T. G., 1971 *Genetics of the evolutionary process*. Columbia University
661 Press.

662 Fabian D. K., Kapun M., Nolte V., Kofler R., Schmidt P. S., *et al.*, 2012 Genome-
663 wide patterns of latitudinal differentiation among populations of *Drosophila*
664 *melanogaster* from North America. *Molecular Ecology* **21**: 4748–4769.

665 Fisher R. A., 1922 On the interpretation of χ^2 from contingency tables, and the
666 calculation of P. *Journal of the Royal Statistical Society*: 87–94.

667 Fiston-Lavier A.-S., Singh N. D., Lipatov M. and D. A. Petrov, 2010 *Drosophila*
668 *melanogaster* recombination rate calculator. *Gene* **463**: 18–20.

669 Futschik A. and C. Schlötterer, 2010 The Next Generation of Molecular Markers
670 From Massively Parallel Sequencing of Pooled DNA Samples. *Genetics* **186**: 207–
671 218.

672 Hasson E. and W. F. Eanes, 1996 Contrasting histories of three gene regions
673 associated with *In(3L)Payne* of *Drosophila melanogaster*. *Genetics* **144**: 1565–
674 1575.

675 Hill W. G. and A. Robertson, 1968 Linkage disequilibrium in finite populations.
676 *Theoret. Appl. Genetics* **38**: 226–231.

677 Hoffmann A. A., Sgrò C. M. and A. R. Weeks, 2004 Chromosomal inversion
678 polymorphisms and adaptation. *Trends in Ecology & Evolution* **19**: 482–488.

679 Hoffmann A. A. and L. H. Rieseberg, 2008 Revisiting the Impact of Inversions in
680 Evolution: From Population Genetic Markers to Drivers of Adaptive Shifts and
681 Speciation? *Annu. Rev. Ecol. Evol. Syst.* **39**: 21–42.

682 Inoue Y., 1979 The fate of polymorphic inversions of *Drosophila melanogaster*
683 transferred to laboratory conditions. *Japanese Journal of Genetics* **54**: 83–96.

684 Inoue Y., Watanabe T. and T. K. Watanabe, 1984 Evolutionary Change of the
685 Chromosomal Polymorphism in *Drosophila melanogaster* Populations. *Evolution*
686 **38**: 753–765.

687 Izquierdo J. I., García-Vázquez E. and B. Villar, 1991 Correlated variation of
688 chromosomal inversion (*3R*)*C* and extra bristles in *Drosophila melanogaster*.
689 *Heredity* **67**: 183–187.

690 Kennison J., 2000 *Preparation and analysis of polytene chromosomes* (W Sullivan, M
691 Ashburner, and RS Hawley, Eds.). *Drosophila protocols*, Cold Spring Harbor.

692 Knibb W. R., Oakeshott J. G. and J. B. Gibson, 1981 Chromosome Inversion
693 Polymorphisms in *Drosophila melanogaster*. I. Latitudinal Clines and Associations
694 Between Inversions in Australasian Populations. *Genetics* **98**: 833–847.

695 Knibb W. R., 1982 Chromosome inversion polymorphisms in *Drosophila*
696 *melanogaster* II. Geographic clines and climatic associations in Australasia, North

697 America and Asia. *Genetica* **58**: 213–221.

698 Kofler R., Orozco-terWengel P., De Maio N., Pandey R. V., Nolte V., *et al.*, 2011

699 PoPoolation: a toolbox for population genetic analysis of next generation

700 sequencing data from pooled individuals. *PLoS ONE* **6**: e15925.

701 Kolaczkowski B., Kern A. D., Holloway A. K. and D. J. Begun, 2011 Genomic

702 differentiation between temperate and tropical Australian populations of

703 *Drosophila melanogaster*. *Genetics* **187**: 245–260.

704 Krimbas C. and J. R. Powell (Eds.), 1992 *Drosophila Inversion Polymorphism*. CRC

705 Press Llc.

706 Landis J. R., Heyman E. R. and G. G. Koch, 1978 Average Partial Association in

707 Three-Way Contingency Tables: A Review and Discussion of Alternative Tests.

708 *International Statistical Review / Revue Internationale de Statistique* **46**: 237–254.

709 Langley C. H., Stevens K., Cardeno C., Lee Y. C. G., Schrider D. R., *et al.*, 2012

710 Genomic variation in natural populations of *Drosophila melanogaster*. *Genetics*

711 **192**: 533–598.

712 Lemeunier F. and S. Aulard, 1992 Inversion polymorphism in *Drosophila*

713 *melanogaster*. In: Krimbas CB, Powell JR (Eds.), *Drosophila Inversion*

714 *Polymorphism*, CRC PressI Llc, pp. 339–405.

715 Levitan M. and W. J. Etges, 2005 Climate change and recent genetic flux in

716 populations of *Drosophila robusta*. *BMC Evol Biol* **5**: 4.

717 Li H. and R. Durbin, 2009 Fast and accurate short read alignment with Burrows-

718 Wheeler transform. *Bioinformatics* **25**: 1754–1760.

719 Li H., Handsaker B., Wysoker A., Fennell T., Ruan J., *et al.*, 1000 Genome Project

720 Data Processing Subgroup, 2009 The Sequence Alignment/Map format and

721 SAMtools. *Bioinformatics* **25**: 2078–2079.

722 Matzkin L. M., Merritt T. J. S., Zhu C.-T. and W. F. Eanes, 2005 The structure and
723 population genetics of the breakpoints associated with the cosmopolitan
724 chromosomal inversion *In(3R)Payne* in *Drosophila melanogaster*. *Genetics* **170**:
725 1143–1152.

726 McPeck M. S. and T. P. Speed, 1995 Modeling interference in genetic
727 recombination. *Genetics* **139**: 1031–1044.

728 Mettler L. E., Voelker R. A. and T. Mukai, 1977 Inversion Clines in Populations of
729 *Drosophila melanogaster*. *Genetics* **87**: 169–176.

730 Navarro A., Betrán E., Barbadilla A. and A. Ruiz, 1997 Recombination and gene flux
731 caused by gene conversion and crossing over in inversion heterokaryotypes.
732 *Genetics* **146**: 695–709.

733 Navarro A., Barbadilla A. and A. Ruiz, 2000 Effect of inversion polymorphism on the
734 neutral nucleotide variability of linked chromosomal regions in *Drosophila*.
735 *Genetics* **155**: 685–698.

736 Orozco-terWengel P., Kapun M., Nolte V., Kofler R., Flatt T. *et al.*, 2012 Adaptation
737 of *Drosophila* to a novel laboratory environment reveals temporally heterogeneous
738 trajectories of selected alleles. *Molecular Ecology* **21**: 4931–4941.

739 Otto S. and T. Day, 2007 *A Biologist's Guide to Mathematical Modeling in Ecology*
740 *and Evolution*. Princeton Library Press, Princeton, New Jersey.

741 Pool J. E., Corbett-Detig R. B., Sugino R. P., Stevens K. A., Cardeno C. M., *et al.*,
742 2012 Population Genomics of sub-saharan *Drosophila melanogaster*: African
743 diversity and non-African admixture. *PLoS Genet* **8**: e1003080.

744 Powell J. R., 1997 *Progress and Prospects in Evolutionary Biology*. Oxford
745 University Press, Oxford.

746 Prevosti A., Serra L., Ribo G., Agudé M., Sagarra E., *et al.*, 1985 The Colonization

747 of *Drosophila subobscura* in Chile. II. Clines in the Chromosomal Arrangements.
748 Evolution **39**: 838–844.

749 Prevosti A., Ribo G., Serra L., Aguadé M., Balaña J., *et al.*, 1988 Colonization of
750 America by *Drosophila subobscura*: Experiment in natural populations that
751 supports the adaptive role of chromosomal-inversion polymorphism. Proc Natl
752 Acad Sci USA **85**: 5597–5600.

753 R Development Core Team, 2009 R: A Language and Environment for Statistical
754 Computing. <http://R-project.org>.

755 Schaeffer S. W. and W. W. Anderson, 2005 Mechanisms of genetic exchange within
756 the chromosomal inversions of *Drosophila pseudoobscura*. Genetics **171**: 1729–
757 1739.

758 Schaeffer S. W., Bhutkar A., McAllister B., Matsuda M., Matzkin L. M., *et al.*, 2008
759 Polytene chromosomal maps of 11 *Drosophila* species: the order of genomic
760 scaffolds inferred from genetic and physical maps. Genetics **179**: 1601.

761 Shin J.-H., Blay S., McNeney B. and J. Graham, 2006 LDheatmap: an R function for
762 graphical display of pairwise linkage disequilibria between single nucleotide
763 polymorphisms. Journal of Statistical Software 16: 1–9.

764 Sturtevant A., 1917 Genetic factors affecting the strength of linkage in *Drosophila*.
765 Proc Natl Acad Sci USA **3**: 555.

766 Wright S. and T. G. Dobzhansky, 1946 Genetics of Natural Populations. XII.
767 Experimental Reproduction of Some of the Changes Caused by Natural Selection
768 in Certain Populations of *Drosophila pseudoobscura*. Genetics 31: 125–156.

769
770
771

772 **Figure Legends**

773 **Figure 1. Nucleotide diversity (π) and genetic differentiation (F_{ST}) for *In(3R)Mo***
774 **and *In(3R)C*.** Line plots showing nucleotide diversity (π) in standard (blue) and
775 inverted (red) chromosomal arrangements; additionally, F_{ST} values (black) show the
776 amount of genetic differentiation between arrangements. (A) *In(3R)Mo* (based on five
777 individuals). (B) *In(3R)C* (based on six individuals). Values for standard arrangement
778 chromosomes (blue) were obtained from comparing three individual chromosomes.
779 Putative boundaries of the three overlapping inversions on *3R* are indicated by
780 vertical black lines: the dashed line represents *In(3R)Mo*, the dotted line *In(3R)P* and
781 the solid line *In(3R)C*.

782

783 **Figure 2. Linkage disequilibrium for *In(3R)Mo* and *In(3R)C*.** Triangular heatmaps
784 showing estimates of r^2 for 5000 randomly sampled SNPs across *3R*. The bottom
785 triangles show the results for inverted arrangements, whereas the top triangles show
786 the standard arrangements (based on three individuals). (A) r^2 plots for *In(3R)Mo*
787 (based on 5 individuals). (B) r^2 plots for *In(3R)C* (based on 6 individuals). The
788 chromosomal position of the three overlapping inversions on *3R* is indicated by a
789 colored line: *In(3R)P* (red), *In(3R)Mo* (blue), and *In(3R)C* (black).

790

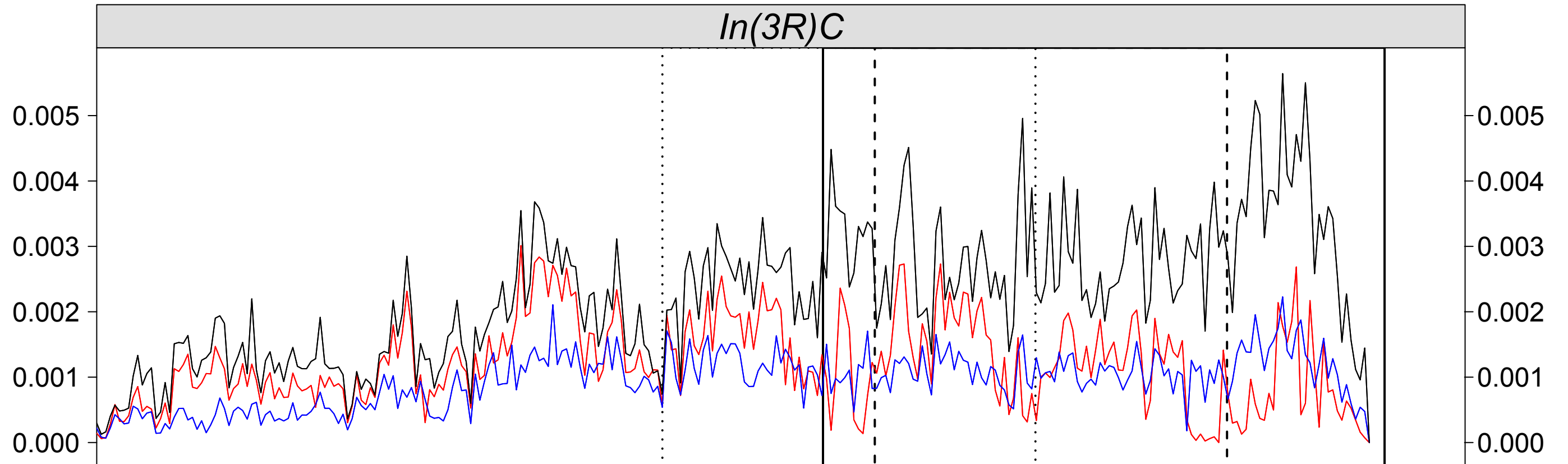
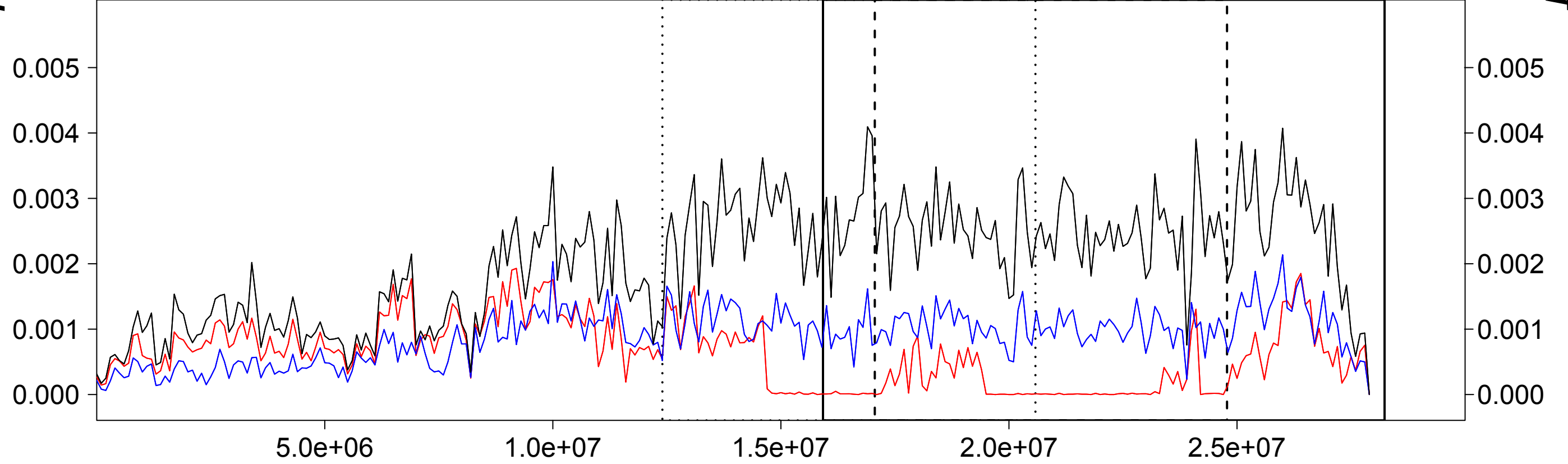
791 **Figure 3. Distribution of fixed SNPs within inversions.** Chromosomal distribution
792 of inversion-specific differences based on a global sample of 167 haplotypes. The
793 number of divergent SNPs is binned in 100-kb non-overlapping sliding windows and
794 plotted along the chromosomal arm carrying the corresponding inversion. Vertical
795 dashed lines indicate the putative inversion breakpoints.

796

797 **Figure 4. Inversion frequency trajectories during experimental evolution.**
798 Inversion frequencies estimated by marker SNPs from Pool-Seq data for the three
799 different replicate populations in each selection regimes (“cold” indicated by dashed
800 and “hot” indicated by solid lines) of our laboratory natural selection experiment. The
801 frequency estimates were calculated by averaging the frequencies of all marker allele
802 for each inversion separately.
803

804 **Table 1. Inversion counts and frequencies.** Counts and frequencies (in parentheses) of six inversions identified by karyotyping in the base
805 population and three replicate populations in each selection regime. The sample size n refers to the number of chromosomes sampled from each
806 population.

Population	n	$In(2L)t$	$In(2R)Ns$	$In(3L)P$	$In(3R)P$	$In(3R)Mo$	$In(3R)E^{807}$
Base	37	12 (0.32)	2 (0.05)	1 (0.03)	4 (0.11)	4 (0.11)	5 (0.14)
cold - R1	36	13 (0.36)	0 (0)	3 (0.08)	3 (0.08)	7 (0.19)	2 (0.06)
cold - R2	45	4 (0.09)	0 (0)	2 (0.04)	0 (0)	12 (0.27)	12 (0.27)
cold - R3	30	10 (0.33)	2 (0.07)	0 (0)	0 (0)	6 (0.2)	3 (0.1)
hot - R1	42	15 (0.36)	0 (0)	2 (0.05)	0 (0)	2 (0.05)	19 (0.45)
hot - R2	44	10 (0.23)	0 (0)	3 (0.07)	2 (0.05)	1 (0.02)	15 (0.34)
hot - R3	41	16 (0.39)	0 (0)	0 (0)	0 (0)	1 (0.02)	17 (0.41)
Sum	275	80	4	11	9	33	73

F_{ST} *In(3R)Mo* F_{ST}

5.0e+06

1.0e+07

1.5e+07

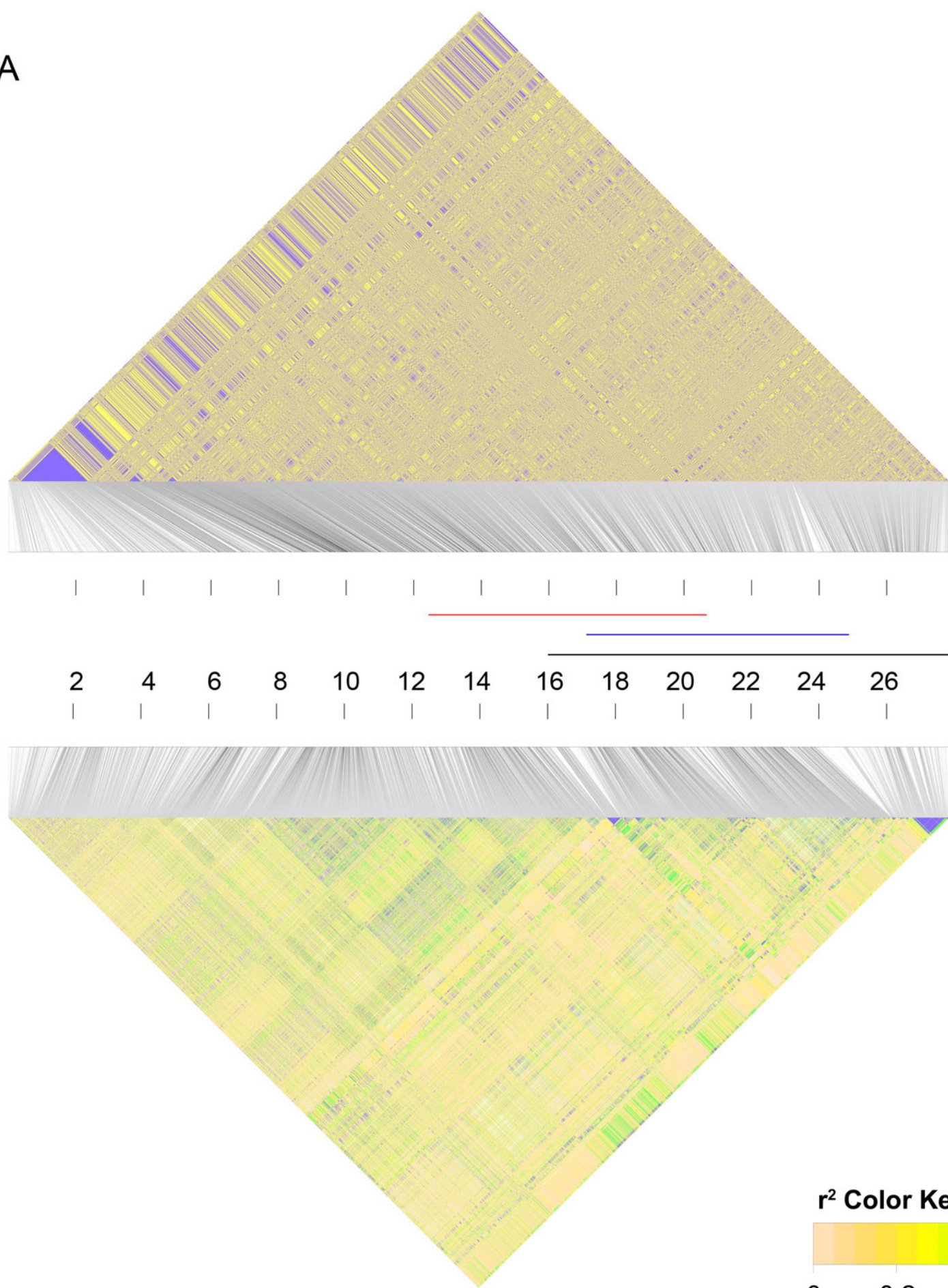
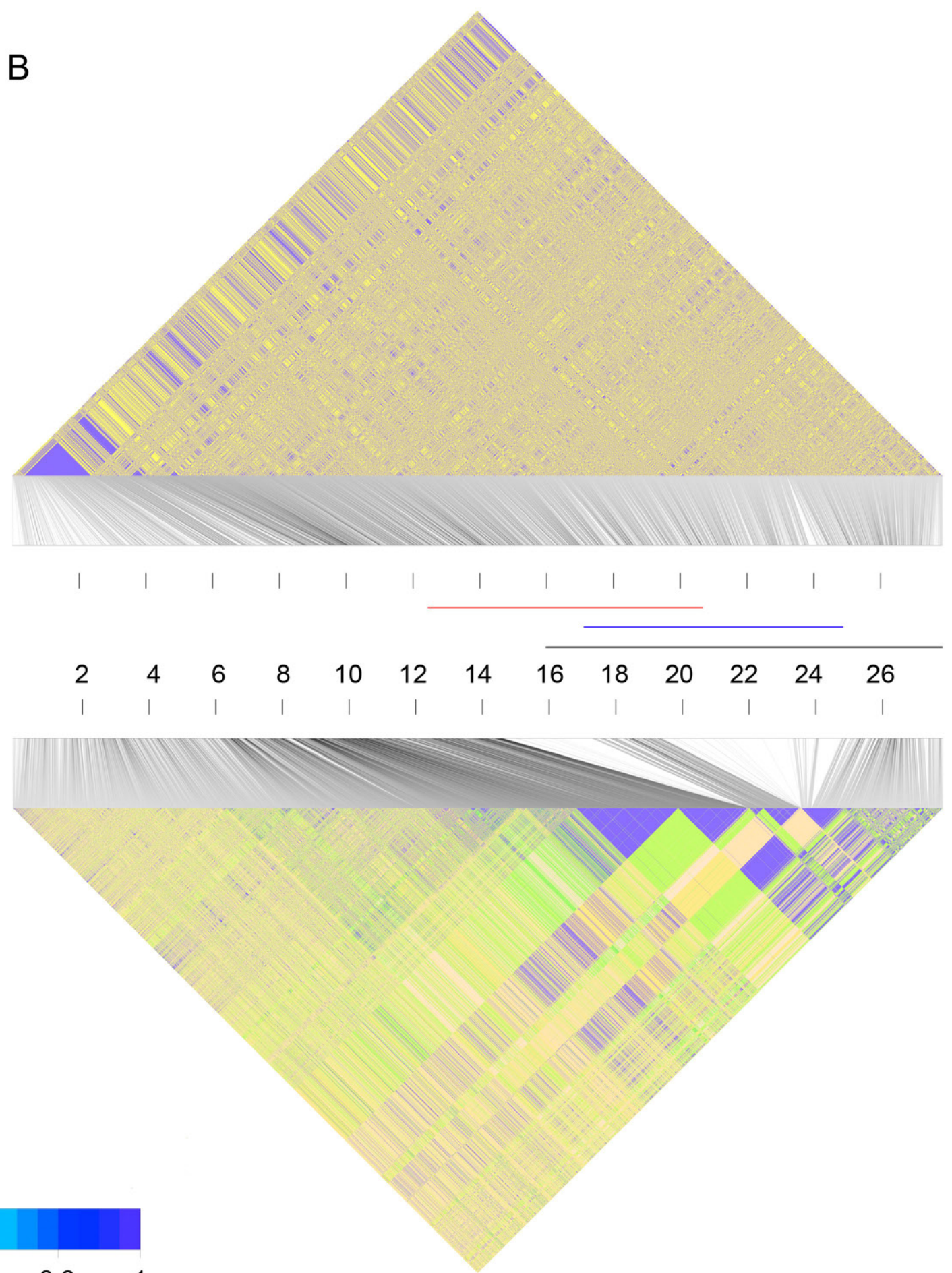
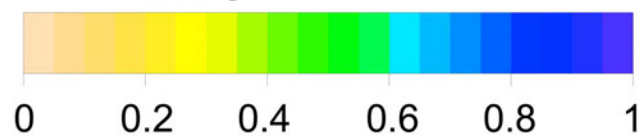
2.0e+07

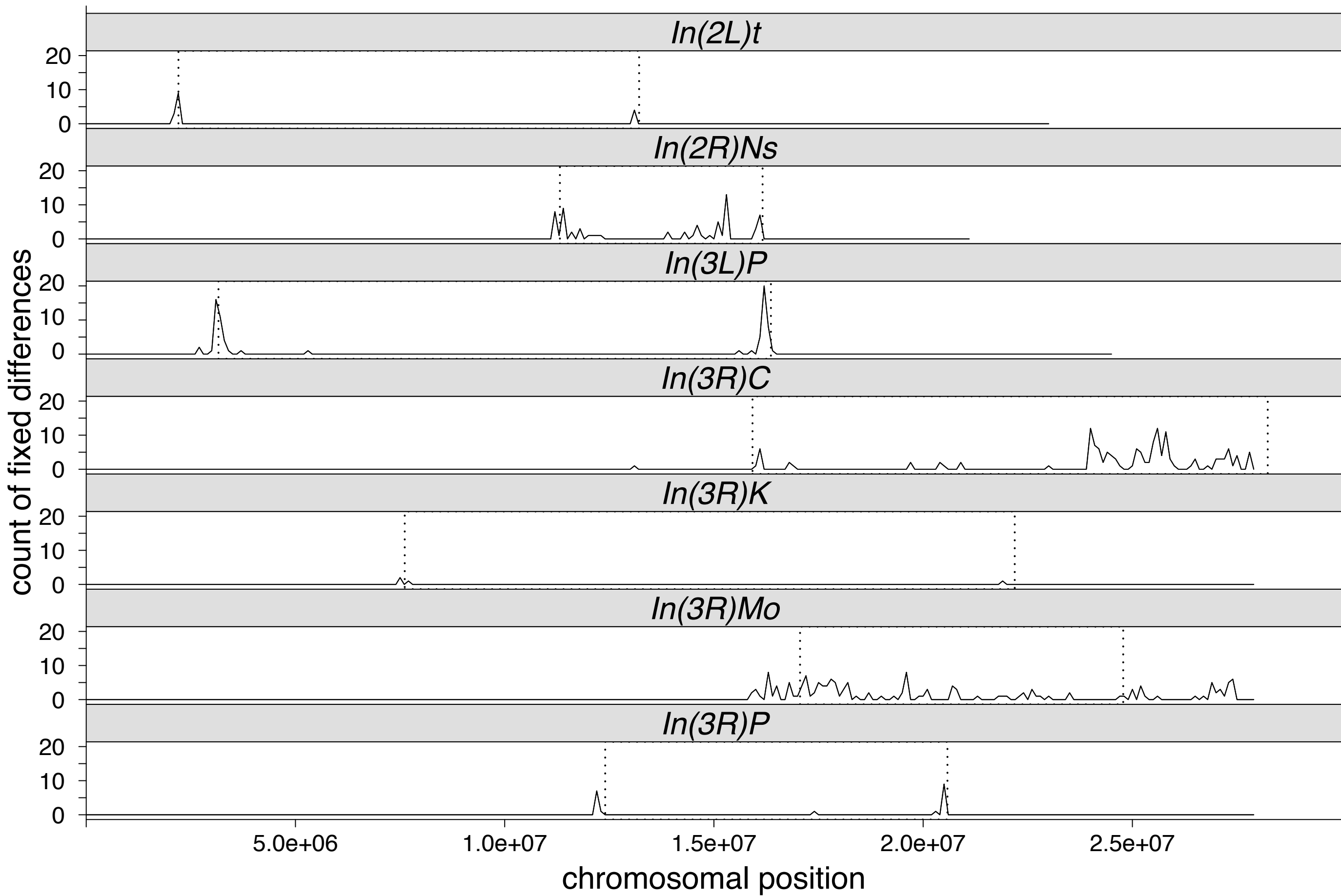
2.5e+07

chromosomal position

A

Chromosomal position (million basepairs)

**B** **r^2 Color Key**



Inversion frequencies

In(2L)t

In(2R)Ns

In(3L)P

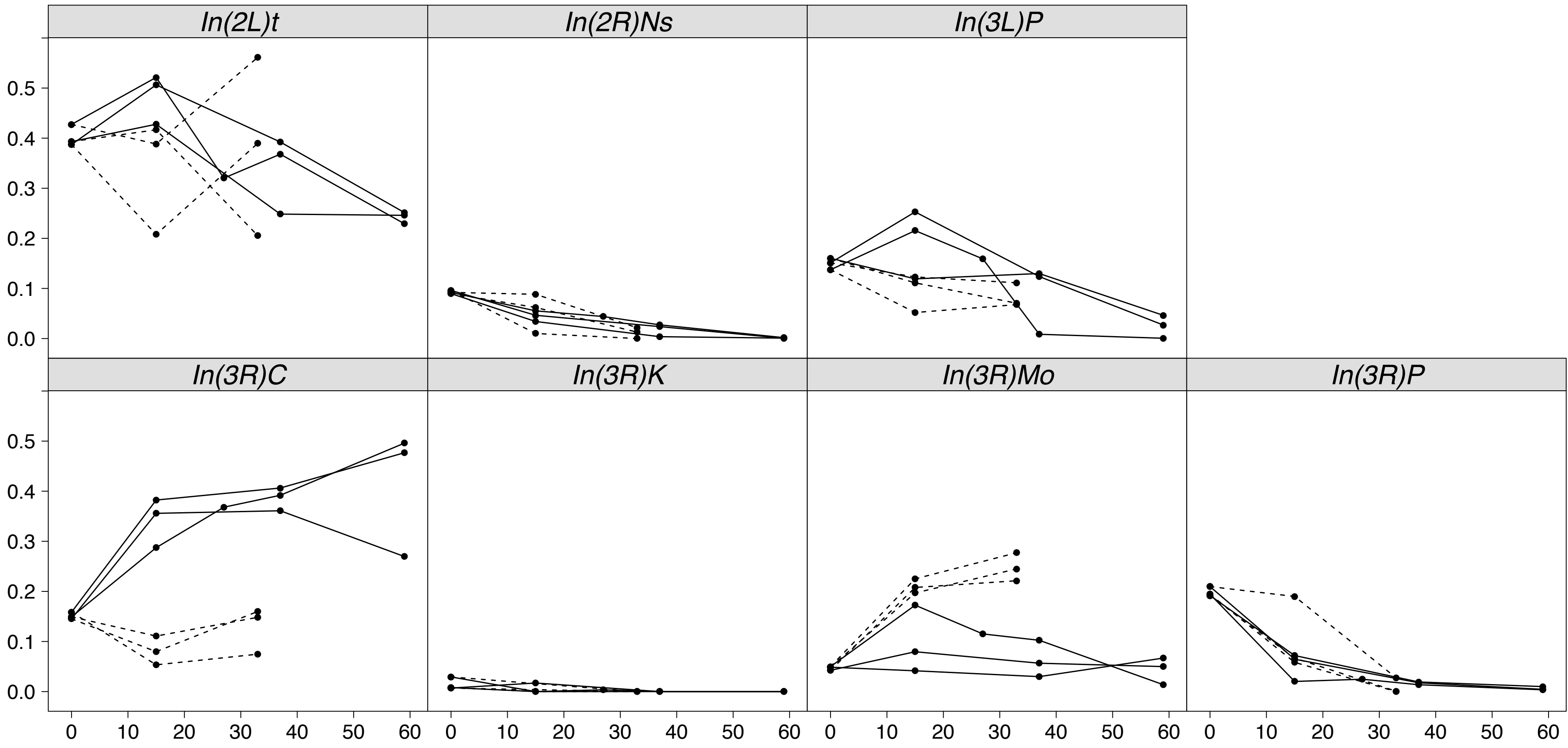
In(3R)C

In(3R)K

In(3R)Mo

In(3R)P

Generations



1	Supporting Information	
2		
3	Estimation of false negative and false positives during haplotype reconstruction	2
4		
5	Number of false positives in inversion-specific fixed differences	3
6		
7	Reliability of using inversion-specific fixed differences as inversion-specific markers	
8	in Pool-Seq data	4
9		
10	Complex patterns of gene flux and genetic variation in overlapping inversions	5
11		
12	References	6
13		
14	Supporting Figures and Tables.....	7
15		
16	Documentation of bioinformatics pipeline.....	48

17

18 Estimation of false negative and false positives during haplotype reconstruction

19 Based on our crossing scheme for chromosomal karyotyping, we developed a novel
20 bioinformatics pipeline to reconstruct sire (male parent) haplotypes from whole-
21 genome-sequenced F1 larvae. As described in the Material and Methods section, we
22 implemented several filtering and stringency thresholds to avoid wrongly typed
23 alleles. Here we describe two methods, which were used to estimate the number of
24 false positives and false negatives among reconstructed haplotypes. First, we sexed
25 sequenced larvae based on cytology and sequencing data: male *Drosophila*
26 individuals are homozygous for the *X* chromosome, which results in (i) large DNA
27 staining intensity differences between autosomes and the *X* in preparations of
28 polytene chromosomes and (ii) large coverage differences between autosomes and the
29 *X* in next-generation sequencing data. With these two methods, we were able to
30 unambiguously identify two male larvae in our dataset. In these individuals, only the
31 maternal copy of the *X* chromosome was sequenced; thus, all SNPs detected on the *X*
32 in these individuals represent sequencing or mapping errors. These data therefore
33 allowed us to estimate the overall false positive rate. For individual number 136
34 (approximately 48-fold autosomal coverage) and individual number 100
35 (approximately 27-fold autosomal coverage) we detected 9 and 13 false positive SNPs
36 respectively, translating into false positive rates of 4×10^{-7} and 5×10^{-7} along the *X*
37 chromosome (approximately 22.4 mb long) for the parameter combinations used in
38 the analysis. Supporting Figure 5 shows the false positive rate for four different
39 parameter combinations for both male individuals. Second, in single individuals
40 sequenced with next-generation sequencing allele frequencies of polymorphic SNPs
41 are distributed around a frequency of 0.5 depending on sequencing depth. However,

42 low coverages inflate the sampling error, which can result in the absence of
43 polymorphic alleles. Given that we sequenced the reference strain used for the
44 crosses, we were able to identify cases among the F1 hybrid sequences for which
45 positions appeared to be fixed for an allele different than the reference. Assuming that
46 the distribution of frequencies caused by sampling error is symmetrical, we were able
47 to obtain false negative rates for our data. Supporting Figure 6 shows the average
48 coverages and false negative rates for each individual at different minimum coverage
49 thresholds. In summary, our results strongly suggest that the haplotype datasets used
50 in our analysis were not affected by high false positive and false negative rates.

51

52 **Number of false positives in inversion-specific fixed differences**

53 In our study we developed a panel of inversion-specific fixed SNP markers, obtained
54 by analyzing karyotype-specific nucleotide variation in an alignment of 167 *D.*
55 *melanogaster* genomes originating from Africa, Europe and North America (see
56 Supporting Table 1). To rule out false positives due to sampling artifacts, we
57 estimated false positive rates using permutations. We randomly assigned individuals
58 as being inverted or non-inverted a 100 times (in the same proportions as in the real
59 data) and counted the number of falsely identified candidates. None of the permuted
60 data resulted in any false positive candidate SNPs.

61 We further tested whether the inversion-specific markers SNPs identified inversion
62 frequency differences more accurately than randomly selected SNPs located within
63 the boundaries of corresponding inversions. We therefore performed CMH tests
64 between the base population and consecutive experimental generations in both
65 selection regimes for each marker SNP separately, as described in Materials and
66 Methods. To obtain a combined result we averaged over all χ^2 values. We then

67 randomly sampled 10,000 times the same number of SNPs as the real marker SNPs
68 and performed CMH tests; for each of these 10,000 sets we counted how often the χ^2
69 values from the random data were larger than for the marker SNPs. By sampling from
70 the tails of this distribution we obtained empirical *P*-value estimates, based on a cut-
71 off defined by the χ^2 value of the real marker SNPs. Under the null hypothesis,
72 inversion-specific alleles would be expected to not perform better in predicting
73 inversion frequencies than randomly drawn samples from within the inversion. The
74 empirical *P*-values from this analysis are shown in Supporting Table 11. We found
75 that our marker SNPs performed significantly better than randomly drawn SNPs for
76 those inversions whose frequencies changed most strongly over time in our selection
77 experiment (i.e., *In(3R)P* and *In(2R)Ns* in both regimes; *In(3R)Mo* in the “cold”
78 regime; and *In(3R)C* in the “hot” regime), but not for inversions whose frequencies
79 changed only weakly or which were segregating at very low baseline frequencies.

80

81 **Reliability of using inversion-specific fixed differences as inversion-specific**
82 **markers in Pool-Seq data**

83 Next, we examined the extent to which our fixed marker SNPs provide accurate
84 estimates of inversion frequencies in our Pool-Seq data. To do so, we compared
85 empirical data based on karyotyping of flies from our laboratory natural selection
86 experiment with inversion frequencies estimated from our Pool-Seq data. Using
87 Fisher’s exact tests (FET) we asked whether inversion frequency counts obtained
88 from karyotyping differ significantly from the average inversion frequency counts as
89 estimated by our inversion-specific SNP markers. None of the 36 tests (6 inversions
90 × 2 treatments × 3 replicates; Supporting Table 9) resulted in *P*-values <0.05.
91 Therefore, our results clearly suggest that our set of inversion-specific marker SNPs is

92 very reliable and robust in terms of accurately estimating inversion frequencies from
93 Pool-Seq datasets.

94

95 **Complex patterns of gene flux and genetic variation in overlapping inversions**

96 The presence of three overlapping inversions on *3R* in our haplotype data provides a
97 unique opportunity for studying genetic exchange between different arrangements.
98 We focused on *In(3R)Mo* which was represented by 5 chromosomes in our dataset.
99 With the exception of two polymorphic regions within the inversion boundaries,
100 *In(3R)Mo* showed almost complete absence of genetic variation within and beyond
101 the inversion boundaries (see Figure 1). We identified two individuals (numbers 96
102 and 100) which carried polymorphisms within the inversion body of *In(3R)Mo* (see
103 Supporting Figure 7A). To further explore the genealogical relationship among all
104 chromosomes with different arrangements in these two polymorphic regions, we
105 reconstructed phylogenetic trees based on π , using only SNPs with unique alleles in
106 individuals 96 and/or 100 (see Supporting Figure 7A-C). Therefore, we constructed
107 distance matrices by calculating average π for all possible chromosome pairs in the
108 sample and used the neighbor-joining method to generate dendrograms using the *R*
109 package ‘ape’ (Paradis *et al.* 2004). We determined the statistical significance of each
110 node by bootstrapping 1000 times, each time randomly drawing a subset corresponding
111 to 10% of all SNPs from the dataset, and then calculated consensus trees using ‘ape’
112 in *R*.

113 Interestingly, in all phylogenies either one or both of these individuals differed
114 significantly from all other *In(3R)Mo* chromosomes. Specifically, in the proximal half
115 of the first polymorphic region, both individuals were highly similar and clustered
116 with the standard arrangement and with the single *In(3R)Payne* individual (see

117 Supporting Figure 7A), whereas individual 100 only clustered with the chromosome
118 carrying *In(3R)Payne* in the distal half (see Supporting Figure 7B). In contrast, in the
119 second region only individual 96 clustered with standard arrangement chromosomes
120 (see Supporting Figure 7C). To further analyze the amount of allele sharing between
121 the different arrangements, we extracted SNPs specific to both individuals and
122 counted how often these alleles segregated in other arrangements. Remarkably, the
123 alleles specific to individual 96 were entirely shared with the standard arrangement
124 but not associated with a single haplotype. Similarly, the majority of alleles (>75 %)
125 specific to individual 100 from the first region were also shared with the standard
126 arrangement. A major proportion of the alleles specific to both individuals was also
127 shared with *In(3R)C* and with the single individual carrying *In(3R)Payne* (see
128 Supporting Table 10). In summary, these findings indicate that the patterns observed
129 within *In(3R)Mo* haplotypes are the result of multiple recent recombination events, at
130 first between different arrangements and subsequently between *In(3R)Mo* haplotypes.

131

132 **References**

133 Paradis E., Claude J. and K. Strimmer, 2004 APE: Analyses of Phylogenetics and
134 Evolution in R language. *Bioinformatics* **20**: 289–290.

135

136

137

138

139

140

141

142 **Supporting Figures and Tables**

143

144 **Supporting Figure 1. Nucleotide diversity (π) and genetic differentiation (F_{ST}) for**

145 ***In(2L)t* and *In(3L)P*.** Line plots showing π averaged in 100-kb non-overlapping

146 sliding windows of individuals with standard (blue) and inverted (red) chromosomal

147 arrangement; F_{ST} values (black) show the amount of genetic differentiation between

148 these arrangements. (A) results for *In(2L)t*, for five individuals of each karyotype. (B)

149 results for *In(3L)P*, for six individuals of each karyotype. In both (A) and (B), the

150 black boxes represent the putative boundaries of the corresponding inversions.

151

152 **Supporting Figure 2. Linkage disequilibrium for *In(2L)t* and *In(3L)P*.** Triangular

153 heatmaps showing the values of pairwise calculations of r^2 for 5000 randomly

154 sampled SNPs across each chromosome. The bottom half shows the results for

155 individuals with the inverted arrangement, whereas the top half shows the results for

156 standard arrangement chromosomes, based on the same number of individuals as for

157 the inverted karyotype. The chromosomal location of each inversion is highlighted as

158 a red line. (A) Plots for *2L*, with *In(2L)t* at the bottom and the standard arrangement at

159 the top (based on 5 individuals). (B) Plots for *3L*, with *In(3L)P* at the bottom and the

160 standard arrangement at the top (based on 4 individuals).

161

162 **Supporting Figure 3. Inversion frequency trajectories during experimental**

163 **evolution.** Box plots showing the allele frequency distributions of inversion-specific

164 SNP markers across different selection regimes (rows; “hot” and “cold”) and replicate

165 populations (columns) in our laboratory natural selection experiment. We used the

166 median of each distribution to estimate inversion frequencies. (A) Results for *In(2L)t*;

167 (B) for *In(2R)Ns*; (C) for *In(3L)P*; (D) for *In(3R)C*; (E) for *In(3R)K*; (F) for *In(3R)Mo*
168 and (G) for *In(3R)Payne*. We performed CMH tests to test for significant frequency
169 differences between generation 0 and consecutive generations in the experimental
170 evolution experiment for each candidate SNP separately. Combined results were
171 obtained by averaging across all *P*-values of all marker SNPs. Green stars indicate
172 significant results between the base population (generation 0) and the corresponding
173 evolved populations at subsequent timepoints during the selection experiment (*
174 $P < 0.05$, ** $P < 0.01$, *** $P < 0.001$).

175

176 **Supporting Figure 4. Inversion frequencies in natural populations.** Box plots
177 showing allele frequencies of inversion specific SNP markers in latitudinal
178 populations from Australia (A; Kolaczowski *et al.* 2011) and North America (B;
179 Fabian *et al.* 2012). We performed Fisher's Exact tests (FET) to test for significant
180 frequency differences between the population at the lowest latitude (i.e., Florida and
181 Queensland, respectively) and all other populations along each cline for each
182 candidate SNP separately. Combined results were obtained by averaging across all *P*-
183 values of all marker SNPs. Green stars indicate significant results for the comparison
184 between the lowest-latitude population and the other populations (* $P < 0.05$, **
185 $P < 0.01$, *** $P < 0.001$).

186

187 **Supporting Figure 5. False positive rates in haplotype reconstruction.** False
188 positive rates estimated for two male F1 hybrids (individuals 100 and 136) for
189 different filtering parameters (minimum allele count and minimum mapping quality),
190 as described in Materials and Methods; also see Supporting Text for further details.

191

192 **Supporting Figure 6. False negative rates in haplotype reconstruction.** Average
193 coverages based on next-generation sequencing data for the reference strain and all 15
194 F1 hybrids (grey line) and false negative rate estimates for different minimum
195 coverage thresholds for each individual separately. See Supporting Text for further
196 details.

197

198 **Supporting Figure 7. Patterns of recombination within *In(3R)Mo*.** The center plot
199 shows π averaged in 100-kb non-overlapping sliding windows for three different
200 combinations of individuals carrying *In(3R)Mo* within the inverted region on *3R*. The
201 orange line represents individuals 80, 129 and 150; the black line the three former
202 individuals plus individual 100; and the grey line individuals 80,129, 150 and 96.

203 Dendrograms were generated from distance matrices based on π calculated for all
204 pairwise comparisons using SNPs with unique alleles in individuals 96 or 100. The
205 chromosomal arrangements of individuals in the trees are color-coded, with *In(3R)Mo*
206 shown in red, *In(3R)C* in green, *In(3R)Payne* in blue and the standard arrangement in
207 black. We used bootstrapping to test for the consistency of the tree topologies.

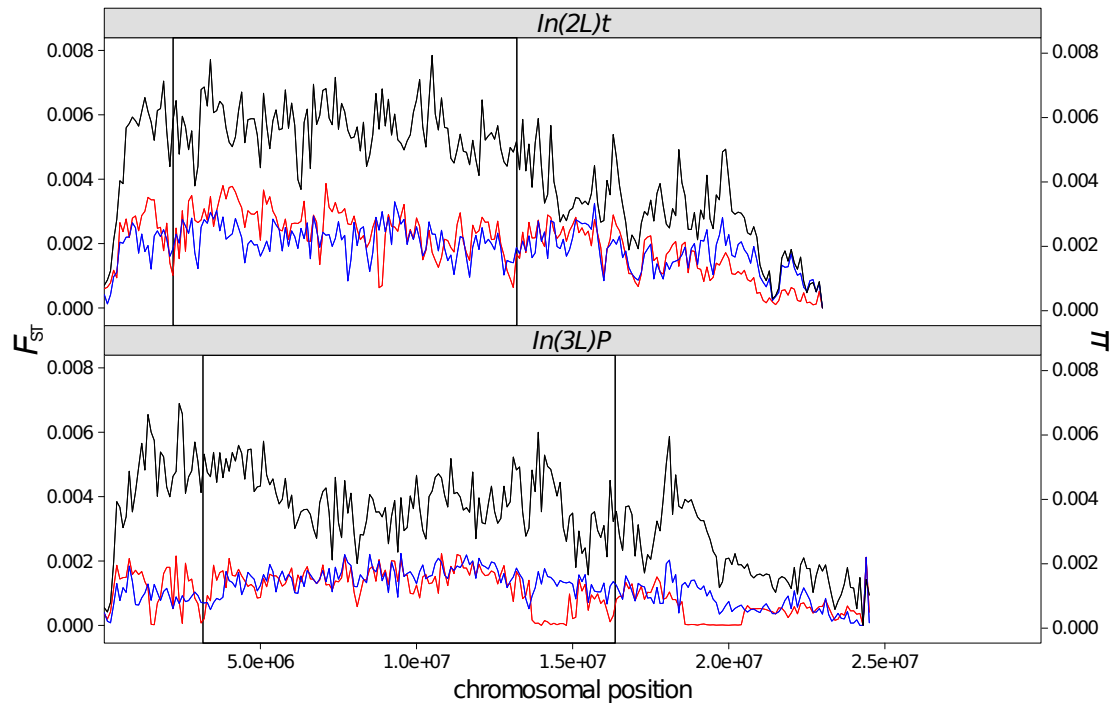
208 Branches with >95% bootstrapping support are indicated with a purple dot. Trees in
209 (A) and (B) are based on SNPs specific for individual 96, whereas (C) is based on
210 SNPs with unique alleles in individual 100. The length of the scale bar in each plot
211 corresponds to $\pi = 0.1$.

212

213

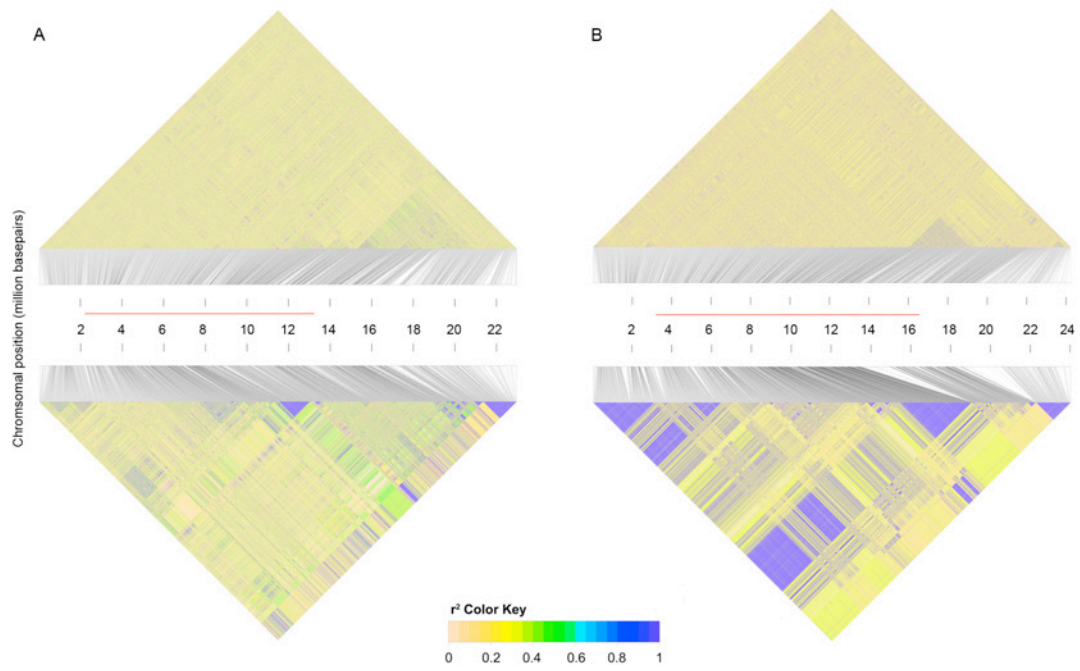
214

215 **Supporting Figure 1**



216

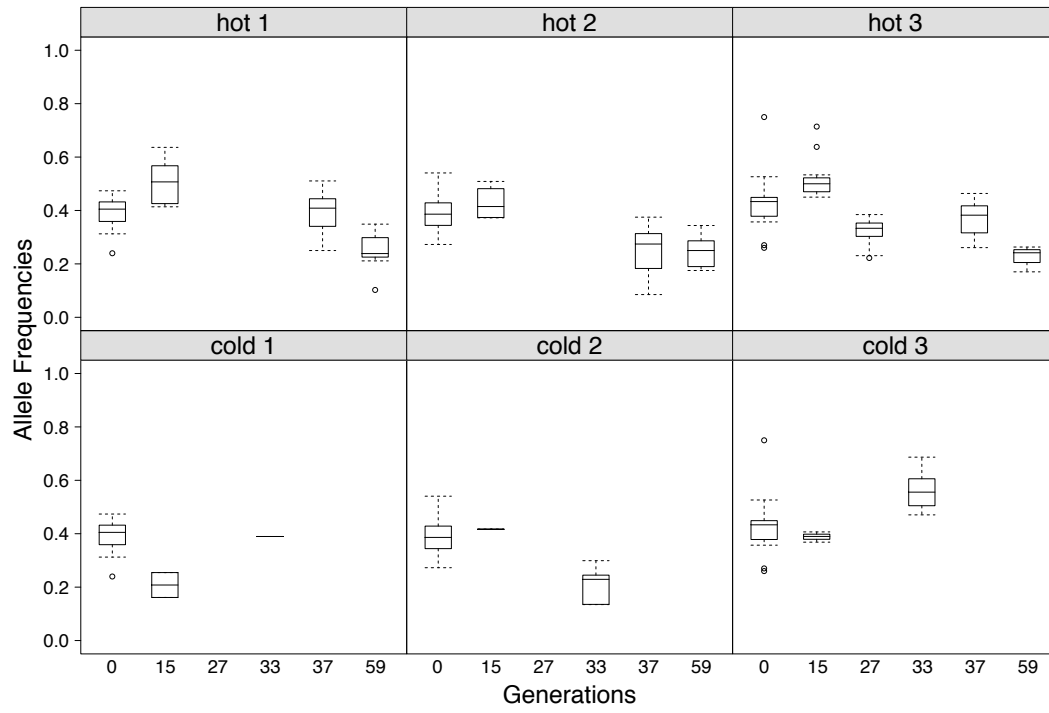
217 **Supporting Figure 2**



218

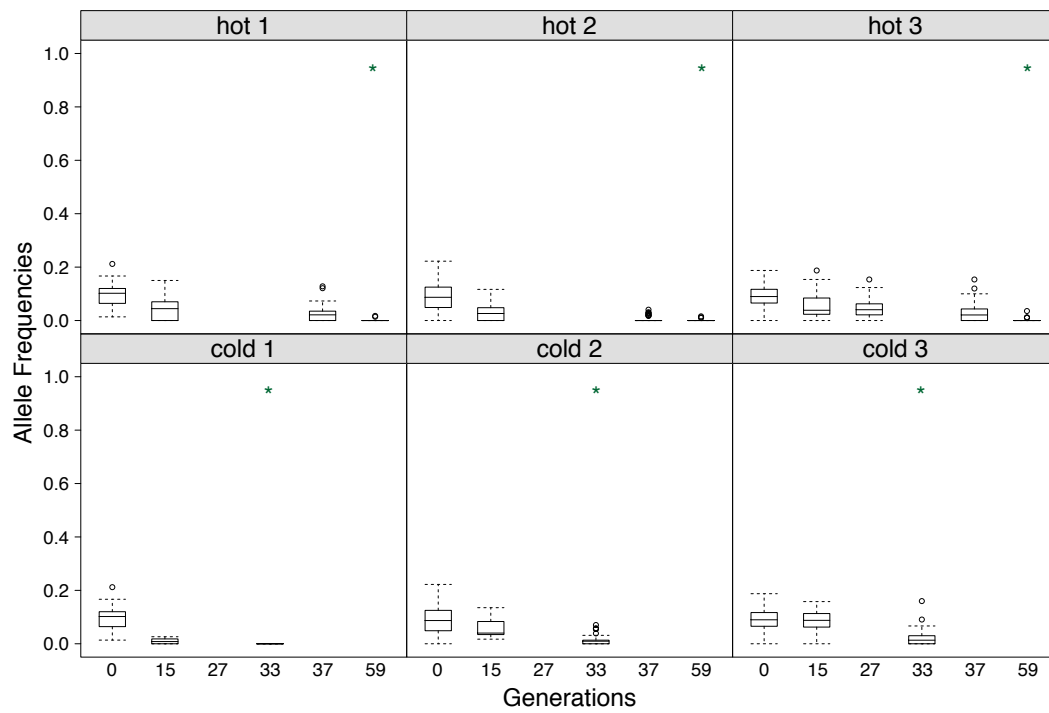
219 **Supporting Figure 3**

220 **A**



221

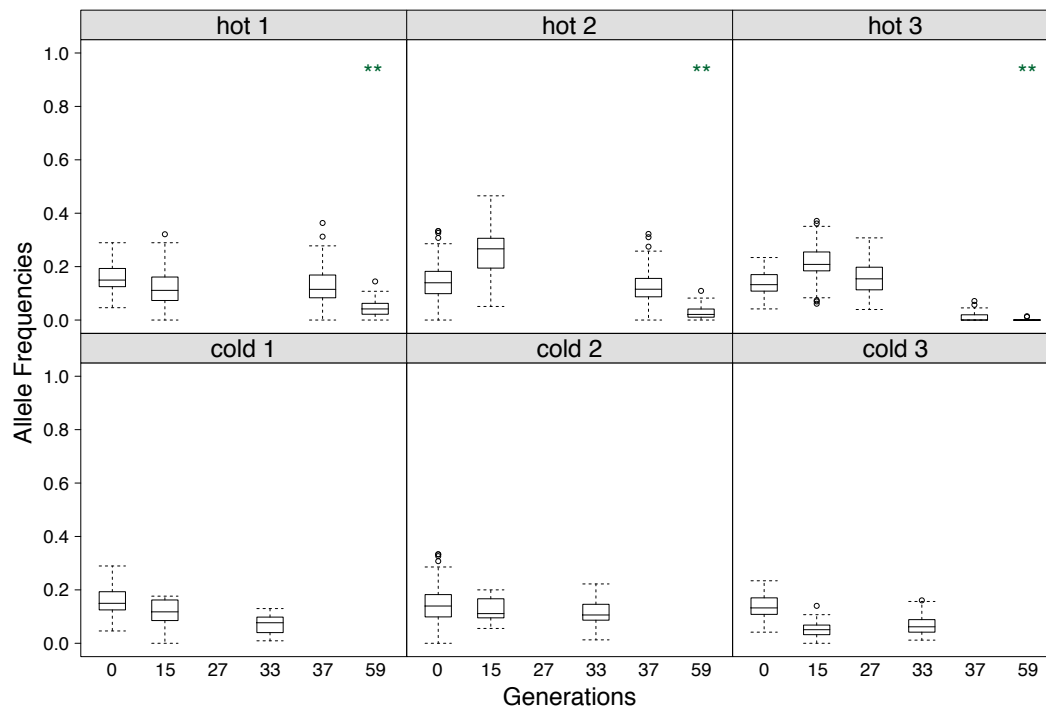
222 **B**



223

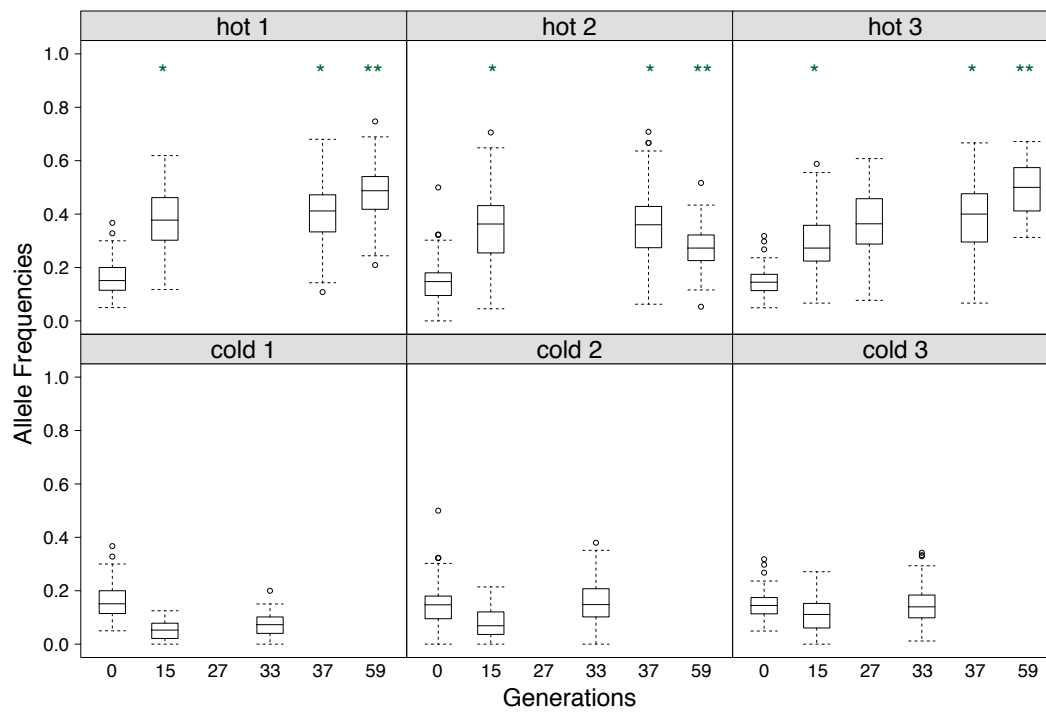
224

225 **C**



226

227 **D**

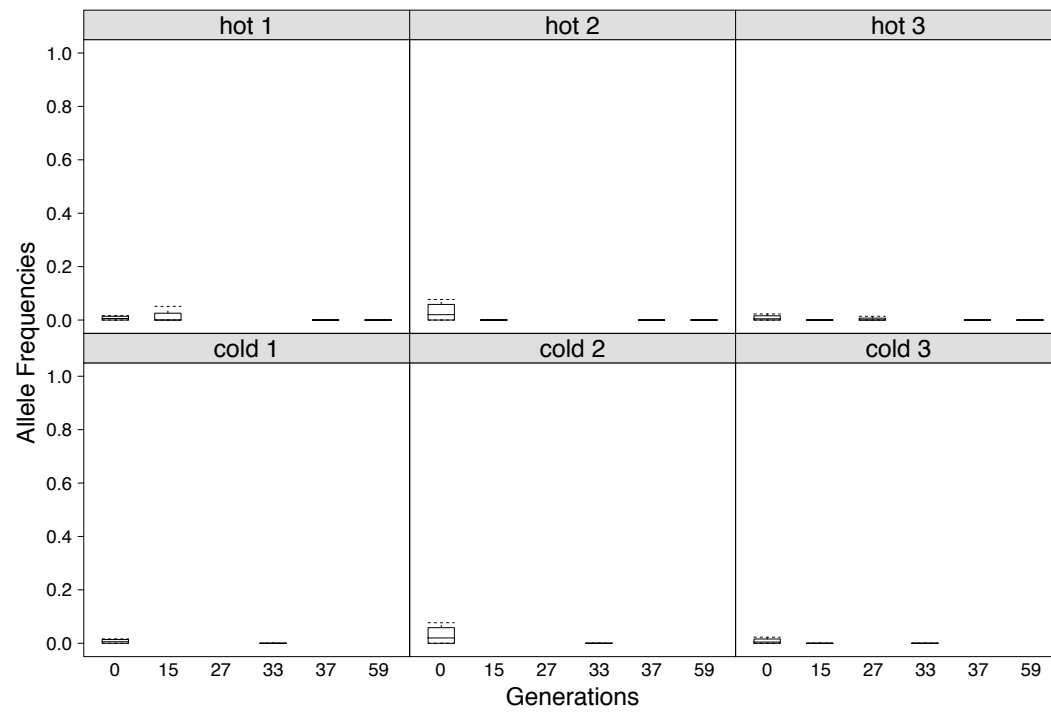


228

229

230

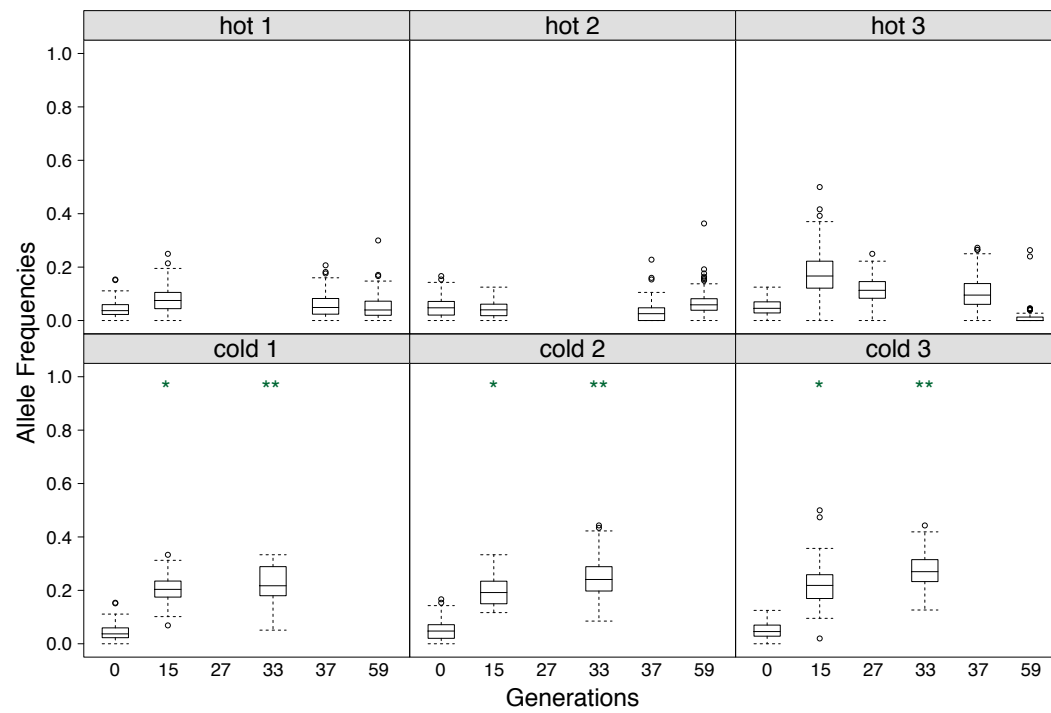
231 **E**



232

233

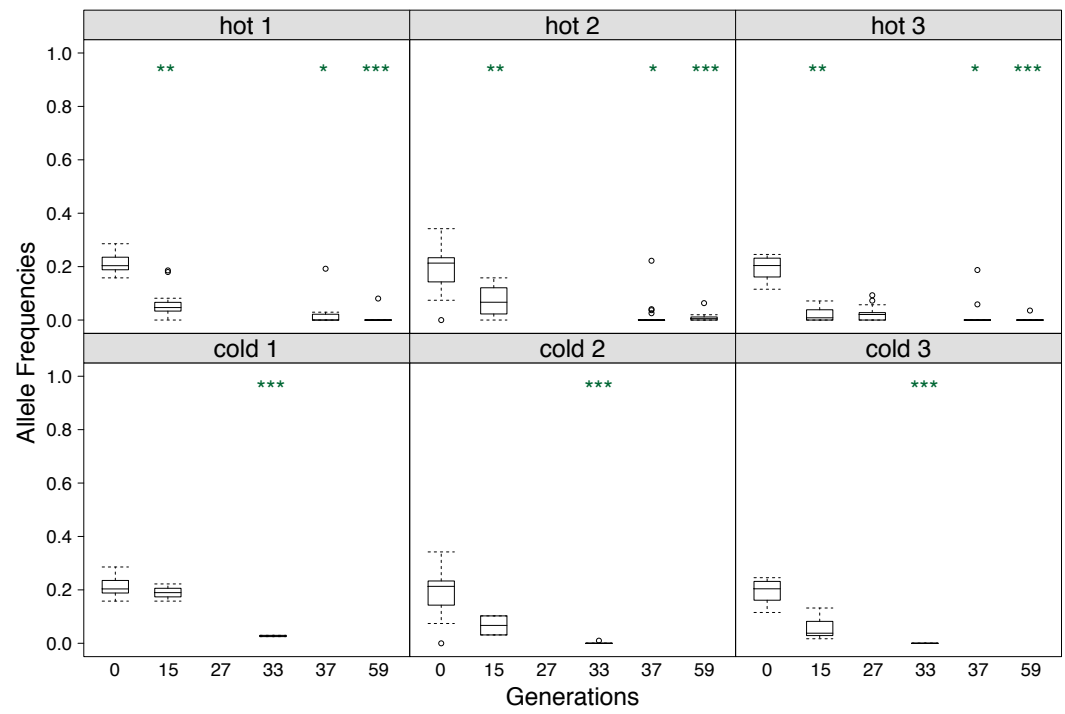
234 **F**



235

236

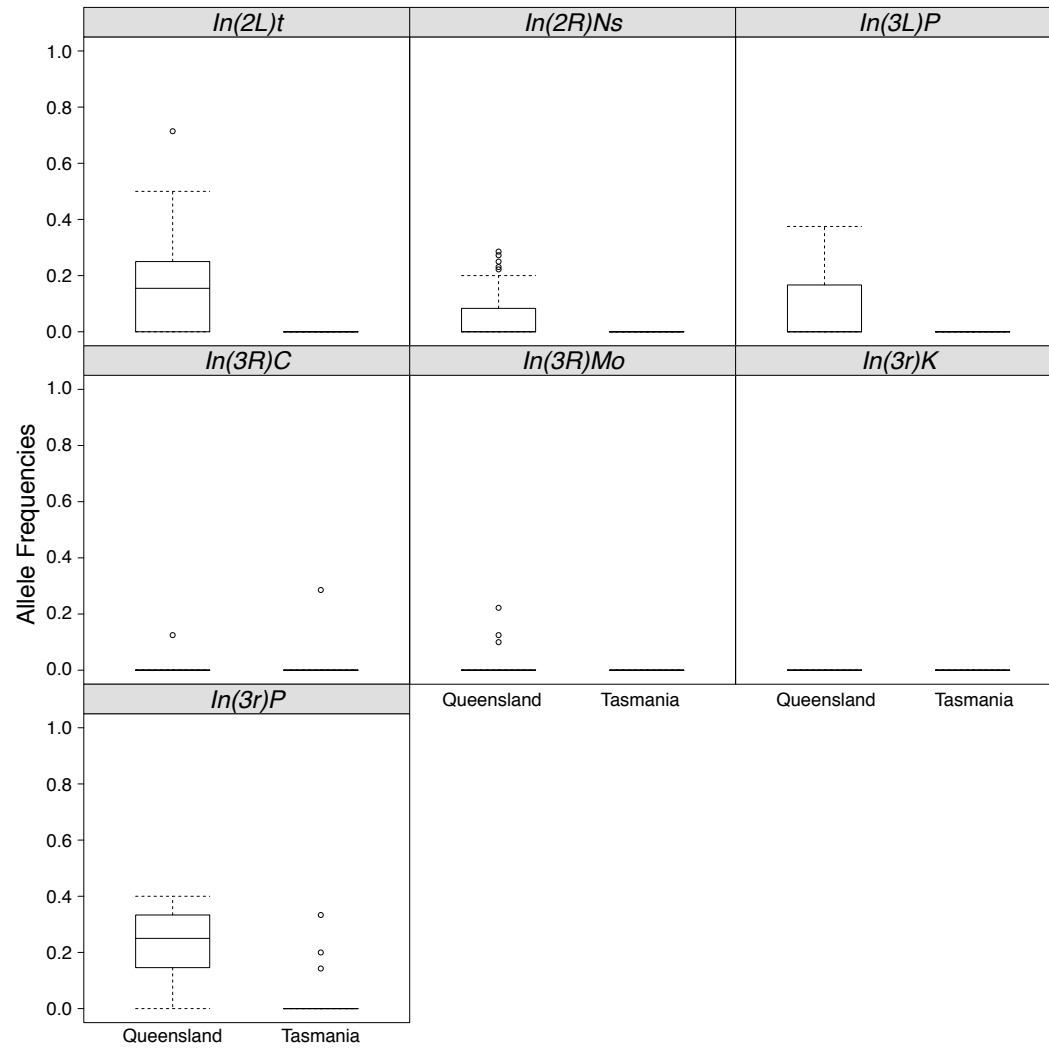
237 **G**



238

239 **Supporting Figure 4**

240 **A**



241

242

243

244

245

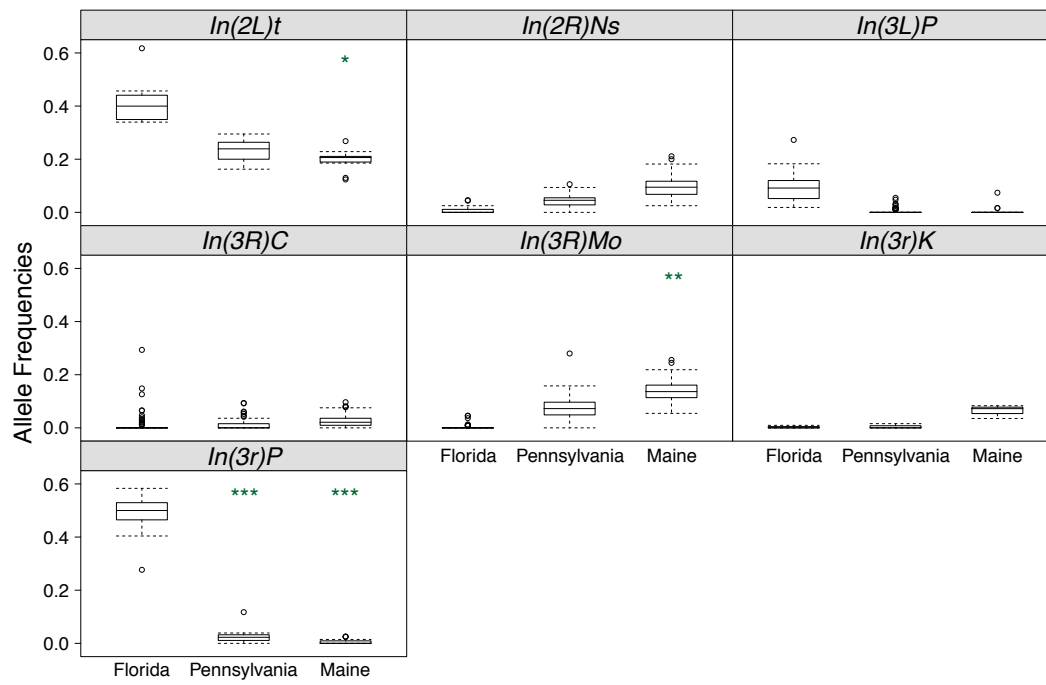
246

247

248

249

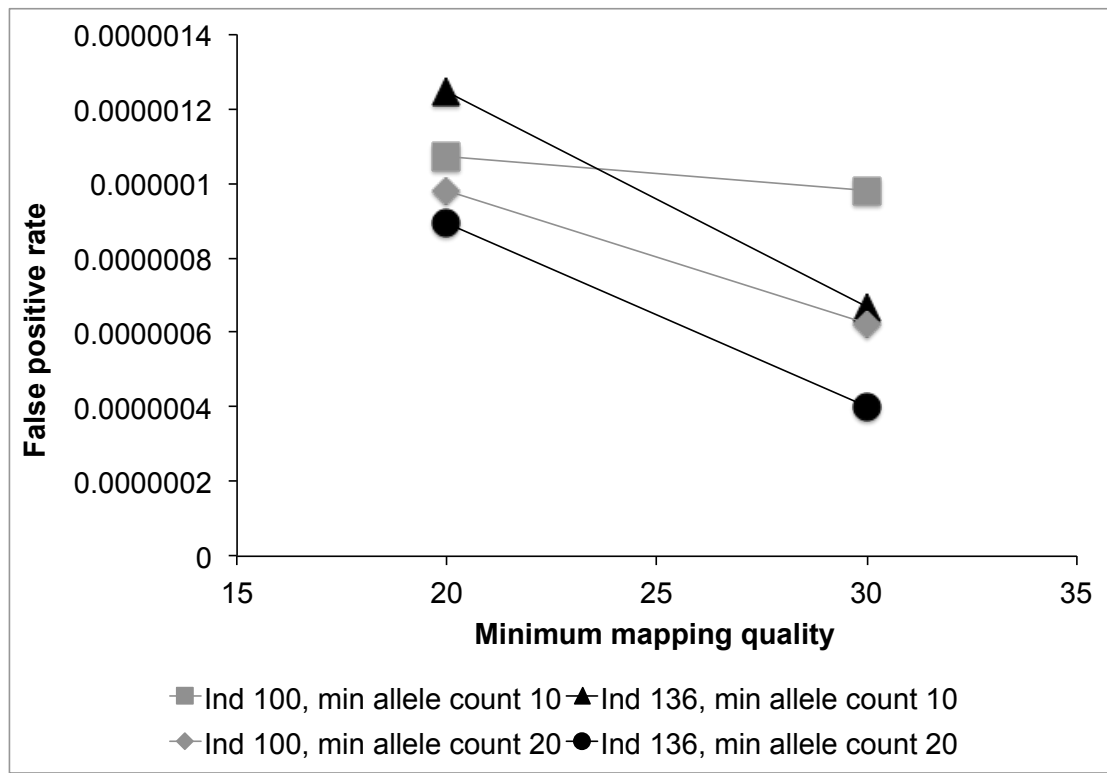
250 **B**



251

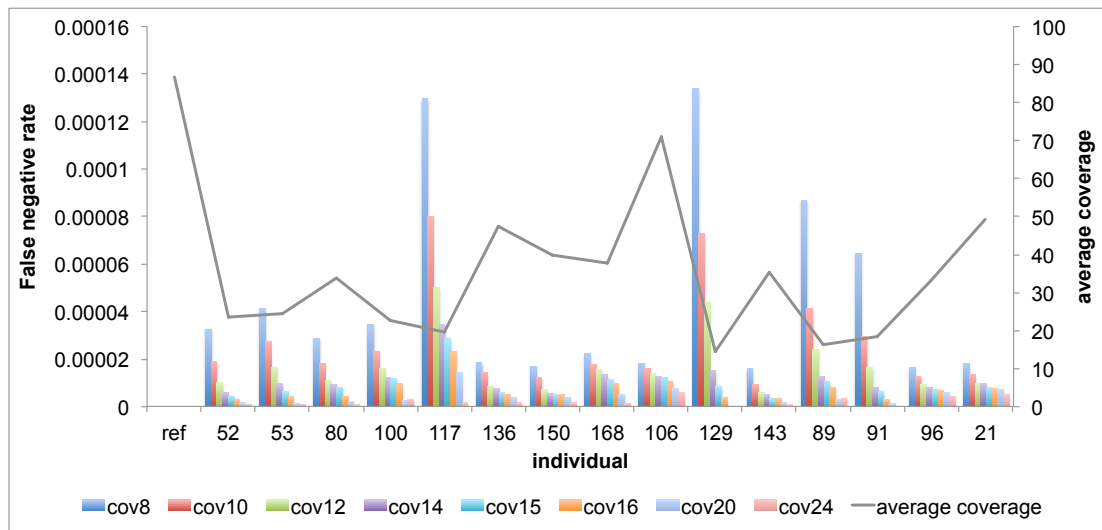
252

253 **Supporting Figure 5**



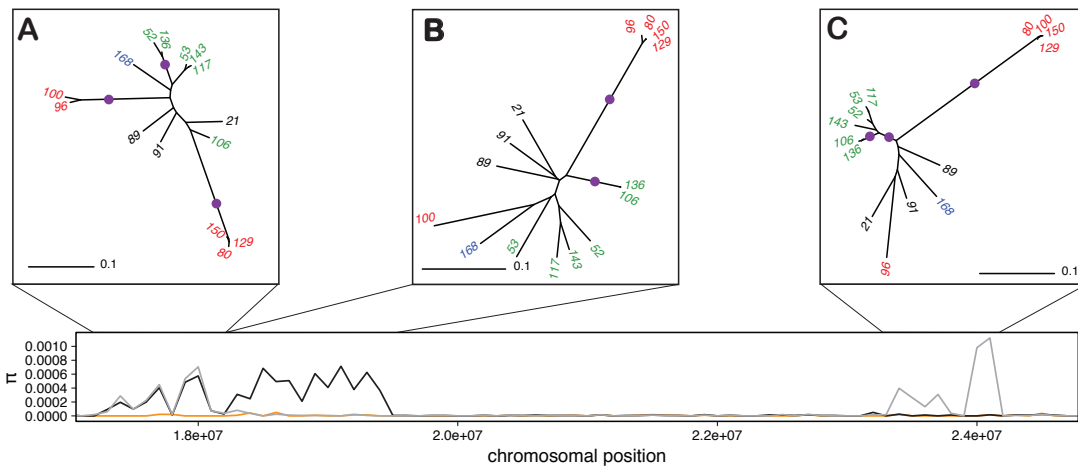
254

255 **Supporting Figure 6**



256

257 **Supporting Figure 7**



258

259

260

262 **Supporting Table 1. Karyotype and sex of sequenced individuals from the experimental evolution experiment.** Number of individual (ID),
 263 selection regime (“hot”, “cold”; replicates (R) 1-3), karyotype and sex of the 15 individuals sequenced from the experimental evolution
 264 experiment. Also see Supporting Table 1 and Materials and Methods.

ID	Regime	<i>In(2L)t</i>	<i>In(2R)Ns</i>	<i>In(3L)P</i>	<i>In(3R)C</i>	<i>In(3R)Mo</i>	<i>In(3R)P</i>	Sex
21	cold-R3	0	1	0	0	0	0	f
52	cold-R2	0	0	0	1	0	0	f
53	cold-R2	0	0	0	1	0	0	f
80	cold-R2	1	0	0	0	1	0	f
89	cold-R2	0	0	1	0	0	0	f
91	cold-R1	0	0	1	0	0	0	f
96	cold-R1	0	0	0	0	1	0	f
100	cold-R1	1	0	0	0	1	0	m
106	hot-R1	1	0	0	1	0	0	f
117	hot-R1	0	0	1	1	0	0	f
129	hot-R1	0	0	0	0	1	0	f
136	hot-R1	1	0	0	1	0	0	m
143	hot-R2	1	0	1	1	0	0	f
150	hot-R2	0	0	0	0	1	0	f
168	hot-R2	0	0	0	0	0	1	f

264 **Supporting Table 2. Individual karyotypes.** Data source, geographic origin, individual number (ID) and karyotype for all 167 individuals
 265 used to identify fixed differences between chromosomal arrangements.

Source	Origin	ID	<i>In(2L)t</i>	<i>In(2R)Ns</i>	<i>In(3L)P</i>	<i>In(3R)C</i>	<i>In(3R)K</i>	<i>In(3R)Mo</i>	<i>In(3R)P</i>
this study	Europe	21	0	1	0	0	0	0	0
this study	Europe	52	0	0	0	1	0	0	0
this study	Europe	53	0	0	0	1	0	0	0
this study	Europe	80	1	0	0	0	0	1	0
this study	Europe	89	0	0	1	0	0	0	0
this study	Europe	91	0	0	1	0	0	0	0
this study	Europe	96	0	0	0	0	0	1	0
this study	Europe	100	1	0	0	0	0	1	0
this study	Europe	106	1	0	0	1	0	0	0
this study	Europe	117	0	0	1	1	0	0	0
this study	Europe	129	0	0	0	0	0	1	0
this study	Europe	136	1	0	0	1	0	0	0
this study	Europe	143	1	0	1	1	0	0	0
this study	Europe	150	0	0	0	0	0	1	0
this study	Europe	168	0	0	0	0	0	0	1
DPGP2	Africa	CK1	0	0	0	0	0	0	1
DPGP2	Africa	CK2	0	0	0	0	0	0	0
DPGP2	Africa	CO1	0	0	0	0	1	0	0
DPGP2	Africa	CO10N	0	0	0	0	1	0	0
DPGP2	Africa	CO13N	0	0	0	0	1	0	0
DPGP2	Africa	CO14	1	0	0	0	0	0	1
DPGP2	Africa	CO15N	0	0	0	0	1	0	0

DPGP2	Africa	CO16	0	0	0	0	1	0	0
DPGP2	Africa	CO2	0	0	0	0	1	0	0
DPGP2	Africa	CO4N	0	0	0	0	1	0	0
DPGP2	Africa	CO8N	0	0	0	0	1	0	0
DPGP2	Africa	CO9N	0	0	0	0	1	0	0
DPGP2	Africa	ED10N	0	0	0	0	0	0	0
DPGP2	Africa	ED2	0	0	0	0	0	0	0
DPGP2	Africa	ED3	0	0	0	0	0	0	0
DPGP2	Africa	ED5N	0	0	0	0	0	0	0
DPGP2	Africa	ED6N	0	0	0	0	0	0	0
DPGP2	Africa	EZ2	1	0	0	0	0	0	0
DPGP2	Africa	EZ25	1	0	0	0	0	0	0
DPGP2	Africa	EZ5N	0	0	0	0	0	0	0
DPGP2	Africa	EZ9N	1	0	0	0	0	0	0
DPGP2	Europe	FR14	0	0	0	0	0	0	0
DPGP2	Europe	FR151	0	0	0	0	0	0	0
DPGP2	Europe	FR180	1	0	0	0	0	0	1
DPGP2	Europe	FR217	0	0	1	0	1	0	0
DPGP2	Europe	FR229	0	0	0	0	0	0	1
DPGP2	Europe	FR310	0	0	0	0	0	1	0
DPGP2	Europe	FR361	0	0	1	0	0	0	1
DPGP2	Europe	FR70	0	0	0	0	0	0	0
DPGP2	Africa	GA125	1	0	0	0	1	0	0
DPGP2	Africa	GA129	1	0	0	0	0	0	0
DPGP2	Africa	GA130	0	0	0	0	0	0	0
DPGP2	Africa	GA132	0	0	0	0	0	0	1
DPGP2	Africa	GA141	1	0	0	0	0	0	0

DPGP2	Africa	GA145	1	0	0	0	0	0	0
DPGP2	Africa	GA160	1	0	0	0	0	0	1
DPGP2	Africa	GA185	0	0	0	0	0	0	1
DPGP2	Africa	GA191	0	0	0	0	0	0	0
DPGP2	Africa	GU10	0	0	0	0	1	0	0
DPGP2	Africa	GU2	0	0	0	0	0	0	0
DPGP2	Africa	GU6	0	0	0	0	1	0	0
DPGP2	Africa	GU7	1	0	0	0	0	0	1
DPGP2	Africa	GU9	0	0	0	0	0	0	1
DPGP2	Africa	KN133N	1	0	0	0	0	0	0
DPGP2	Africa	KN20N	0	0	0	0	1	0	0
DPGP2	Africa	KN34	0	0	0	0	0	0	0
DPGP2	Africa	KN35	1	0	0	0	0	0	0
DPGP2	Africa	KN6	0	0	0	0	0	0	0
DPGP2	Africa	KR39	1	0	0	0	0	0	0
DPGP2	Africa	KR42	1	1	0	0	0	0	0
DPGP2	Africa	KR4N	1	0	0	0	0	0	0
DPGP2	Africa	KR7	1	0	0	0	0	0	0
DPGP2	Africa	KT1	0	0	0	0	0	0	0
DPGP2	Africa	KT6	0	1	0	0	0	0	0
DPGP2	Africa	NG10N	1	0	1	0	0	0	1
DPGP2	Africa	NG1N	1	1	0	0	1	0	0
DPGP2	Africa	NG3N	1	0	1	0	0	0	0
DPGP2	Africa	NG6N	0	0	0	0	0	0	0
DPGP2	Africa	NG7	0	0	0	0	0	0	0
DPGP2	Africa	NG9	1	1	1	0	0	0	0
DPGP2	Africa	RC1	0	0	0	0	0	0	0

DPGP2	Africa	RC5	0	0	0	0	0	0	0
DPGP2	Africa	RG10	0	0	0	0	0	0	0
DPGP2	Africa	RG11N	0	0	0	0	0	0	0
DPGP2	Africa	RG13N	0	0	0	0	0	0	0
DPGP2	Africa	RG15	0	0	0	0	0	0	0
DPGP2	Africa	RG18N	0	0	0	0	0	0	1
DPGP2	Africa	RG19	0	0	0	0	0	0	0
DPGP2	Africa	RG2	0	0	0	0	0	0	0
DPGP2	Africa	RG21N	0	0	0	0	0	0	0
DPGP2	Africa	RG22	0	0	0	0	0	0	0
DPGP2	Africa	RG24	0	0	0	0	0	0	0
DPGP2	Africa	RG25	0	0	0	0	0	0	1
DPGP2	Africa	RG28	0	0	0	0	0	0	0
DPGP2	Africa	RG3	1	1	0	0	0	0	0
DPGP2	Africa	RG32N	0	0	0	0	0	0	0
DPGP2	Africa	RG33	0	0	0	0	0	0	0
DPGP2	Africa	RG34	0	0	0	0	0	0	0
DPGP2	Africa	RG35	0	0	0	0	0	0	0
DPGP2	Africa	RG36	1	0	0	0	0	0	0
DPGP2	Africa	RG37N	1	0	0	0	0	0	0
DPGP2	Africa	RG38N	0	0	0	0	0	0	0
DPGP2	Africa	RG39	0	0	0	0	0	0	0
DPGP2	Africa	RG4N	0	0	0	0	0	0	0
DPGP2	Africa	RG5	0	0	0	0	0	0	1
DPGP2	Africa	RG6N	0	0	0	0	0	0	0
DPGP2	Africa	RG7	0	0	0	0	0	0	0
DPGP2	Africa	RG8	0	0	0	0	0	0	0

DPGP2	Africa	RG9	0	0	0	0	0	0	1
DPGP2	Africa	SP173	0	0	0	0	0	0	0
DPGP2	Africa	SP188	0	0	0	0	0	0	0
DPGP2	Africa	SP221	1	1	0	0	0	0	0
DPGP2	Africa	SP235	0	0	0	0	0	0	0
DPGP2	Africa	SP241	0	0	0	0	0	0	0
DPGP2	Africa	SP254	0	0	0	0	0	0	0
DPGP2	Africa	SP80	0	0	0	0	0	0	0
DPGP2	Africa	TZ10	1	0	0	0	0	0	0
DPGP2	Africa	TZ14	1	0	0	0	1	0	0
DPGP2	Africa	TZ8	1	0	0	0	0	0	0
DPGP2	Africa	UG19	0	0	0	0	0	0	0
DPGP2	Africa	UG28N	0	0	0	0	0	0	0
DPGP2	Africa	UG5N	0	0	0	0	0	0	0
DPGP2	Africa	UG7	0	0	0	0	0	0	0
DPGP2	Africa	UM118	1	0	0	0	0	0	0
DPGP2	Africa	UM37	0	0	0	0	1	0	0
DPGP2	Africa	UM526	1	0	0	0	0	0	0
DPGP2	Africa	ZI261	0	0	0	0	0	0	0
DPGP2	Africa	ZI268	0	0	0	0	0	0	0
DPGP2	Africa	ZI468	0	0	0	0	0	0	0
DPGP2	Africa	ZI91	0	0	0	0	0	0	0
DPGP2	Africa	ZL130	0	0	0	0	0	0	0
DPGP2	Africa	ZO65	1	1	0	0	0	0	0
DPGP2	Africa	ZS11	1	0	0	0	0	0	0
DPGP2	Africa	ZS37	0	0	0	0	1	0	0
DPGP2	Africa	ZS5	0	1	0	0	0	0	0

DPGP	North America	RAL-301	1	0	0	0	0	0	0
DPGP	North America	RAL-303	0	0	0	0	0	0	0
DPGP	North America	RAL-304	0	1	0	0	0	0	0
DPGP	North America	RAL-306	0	0	0	0	0	0	0
DPGP	North America	RAL-307	0	0	0	0	0	0	0
DPGP	North America	RAL-313	1	0	0	0	0	0	0
DPGP	North America	RAL-315	0	0	0	0	0	0	0
DPGP	North America	RAL-324	0	0	0	0	0	1	0
DPGP	North America	RAL-335	0	0	0	0	0	0	0
DPGP	North America	RAL-357	0	0	0	0	0	0	0
DPGP	North America	RAL-358	1	0	0	0	0	1	0
DPGP	North America	RAL-360	0	0	0	0	0	0	0
DPGP	North America	RAL-362	0	0	0	0	0	0	0
DPGP	North America	RAL-365	0	0	0	0	0	0	0
DPGP	North America	RAL-375	0	0	0	0	0	0	0
DPGP	North America	RAL-379	0	0	0	0	0	0	0
DPGP	North America	RAL-380	0	0	0	0	0	0	0
DPGP	North America	RAL-391	0	0	0	0	0	0	0
DPGP	North America	RAL-399	0	0	0	0	0	0	0
DPGP	North America	RAL-427	0	0	0	0	0	0	0
DPGP	North America	RAL-437	0	0	0	0	0	1	0
DPGP	North America	RAL-486	0	0	0	0	0	0	0
DPGP	North America	RAL-514	0	0	0	0	0	0	0
DPGP	North America	RAL-517	0	0	0	0	0	0	0
DPGP	North America	RAL-555	0	0	0	0	0	1	0
DPGP	North America	RAL-639	0	0	0	0	0	0	0
DPGP	North America	RAL-705	0	0	0	0	0	0	0

DPGP	North America	RAL-707	0	0	0	0	0	1	0
DPGP	North America	RAL-714	0	0	0	0	0	1	0
DPGP	North America	RAL-730	0	0	0	0	0	0	0
DPGP	North America	RAL-732	0	0	0	0	1	0	0
DPGP	North America	RAL-765	0	0	0	0	0	0	0
DPGP	North America	RAL-774	0	0	0	0	0	0	0
DPGP	North America	RAL-786	0	0	0	0	0	0	1
DPGP	North America	RAL-799	0	0	0	0	0	0	0
DPGP	North America	RAL-820	0	0	0	0	0	1	0
DPGP	North America	RAL-852	0	1	0	0	0	0	0

267 **Supporting Table 3. Inversion-specific marker alleles.** Chromosomal position and
 268 inversion-specific allele for the fixed differences between the corresponding inversion
 269 and all other chromosomal arrangements, based on 167 chromosomes.

Inversion	Chromosome	Position	Allele
<i>In(2L)t</i>	2L	2166548	A
<i>In(2L)t</i>	2L	2166622	G
<i>In(2L)t</i>	2L	2166626	A
<i>In(2L)t</i>	2L	2204678	A
<i>In(2L)t</i>	2L	2209048	C
<i>In(2L)t</i>	2L	2214322	T
<i>In(2L)t</i>	2L	2225369	T
<i>In(2L)t</i>	2L	2226971	G
<i>In(2L)t</i>	2L	2233906	A
<i>In(2L)t</i>	2L	2234101	A
<i>In(2L)t</i>	2L	2246686	T
<i>In(2L)t</i>	2L	2255218	A
<i>In(2L)t</i>	2L	13139098	C
<i>In(2L)t</i>	2L	13155257	T
<i>In(2L)t</i>	2L	13172139	T
<i>In(2L)t</i>	2L	13186585	A
<i>In(2R)Ns</i>	2R	11279637	A
<i>In(2R)Ns</i>	2R	11291326	A
<i>In(2R)Ns</i>	2R	11291656	A
<i>In(2R)Ns</i>	2R	11294553	A
<i>In(2R)Ns</i>	2R	11295105	A
<i>In(2R)Ns</i>	2R	11295408	A
<i>In(2R)Ns</i>	2R	11297771	T
<i>In(2R)Ns</i>	2R	11298425	C
<i>In(2R)Ns</i>	2R	11363601	T
<i>In(2R)Ns</i>	2R	11416627	T
<i>In(2R)Ns</i>	2R	11416743	G
<i>In(2R)Ns</i>	2R	11428502	G
<i>In(2R)Ns</i>	2R	11452011	C
<i>In(2R)Ns</i>	2R	11453509	T
<i>In(2R)Ns</i>	2R	11459978	G
<i>In(2R)Ns</i>	2R	11467228	T
<i>In(2R)Ns</i>	2R	11470424	T
<i>In(2R)Ns</i>	2R	11471637	T
<i>In(2R)Ns</i>	2R	11620344	A
<i>In(2R)Ns</i>	2R	11685989	T
<i>In(2R)Ns</i>	2R	11817613	A
<i>In(2R)Ns</i>	2R	11818383	T
<i>In(2R)Ns</i>	2R	11826149	T

<i>In(2R)Ns</i>	2R	12007749	A
<i>In(2R)Ns</i>	2R	12154859	A
<i>In(2R)Ns</i>	2R	12250521	T
<i>In(2R)Ns</i>	2R	12394846	G
<i>In(2R)Ns</i>	2R	13942780	A
<i>In(2R)Ns</i>	2R	13944397	C
<i>In(2R)Ns</i>	2R	14352759	A
<i>In(2R)Ns</i>	2R	14362949	T
<i>In(2R)Ns</i>	2R	14582447	T
<i>In(2R)Ns</i>	2R	14633978	T
<i>In(2R)Ns</i>	2R	14641278	A
<i>In(2R)Ns</i>	2R	14672926	A
<i>In(2R)Ns</i>	2R	14674348	T
<i>In(2R)Ns</i>	2R	14735385	G
<i>In(2R)Ns</i>	2R	14995376	T
<i>In(2R)Ns</i>	2R	15117841	T
<i>In(2R)Ns</i>	2R	15122558	G
<i>In(2R)Ns</i>	2R	15124138	T
<i>In(2R)Ns</i>	2R	15154801	A
<i>In(2R)Ns</i>	2R	15160191	A
<i>In(2R)Ns</i>	2R	15289938	G
<i>In(2R)Ns</i>	2R	15303213	T
<i>In(2R)Ns</i>	2R	15303225	A
<i>In(2R)Ns</i>	2R	15335793	T
<i>In(2R)Ns</i>	2R	15339141	T
<i>In(2R)Ns</i>	2R	15339337	T
<i>In(2R)Ns</i>	2R	15344384	A
<i>In(2R)Ns</i>	2R	15345300	T
<i>In(2R)Ns</i>	2R	15348825	A
<i>In(2R)Ns</i>	2R	15364662	C
<i>In(2R)Ns</i>	2R	15364670	C
<i>In(2R)Ns</i>	2R	15366984	A
<i>In(2R)Ns</i>	2R	15367369	A
<i>In(2R)Ns</i>	2R	15370164	A
<i>In(2R)Ns</i>	2R	16023748	T
<i>In(2R)Ns</i>	2R	16071561	T
<i>In(2R)Ns</i>	2R	16073117	T
<i>In(2R)Ns</i>	2R	16100012	T
<i>In(2R)Ns</i>	2R	16116600	A
<i>In(2R)Ns</i>	2R	16117724	T
<i>In(2R)Ns</i>	2R	16152311	C
<i>In(2R)Ns</i>	2R	16152687	G
<i>In(2R)Ns</i>	2R	16160042	T
<i>In(2R)Ns</i>	2R	16163328	T
<i>In(3L)P</i>	3L	2759715	C
<i>In(3L)P</i>	3L	2760784	T

<i>In(3L)P</i>	3L	3054925	C
<i>In(3L)P</i>	3L	3133022	G
<i>In(3L)P</i>	3L	3135682	C
<i>In(3L)P</i>	3L	3142231	A
<i>In(3L)P</i>	3L	3145702	T
<i>In(3L)P</i>	3L	3148304	A
<i>In(3L)P</i>	3L	3152282	C
<i>In(3L)P</i>	3L	3156337	A
<i>In(3L)P</i>	3L	3165913	A
<i>In(3L)P</i>	3L	3172232	A
<i>In(3L)P</i>	3L	3172572	A
<i>In(3L)P</i>	3L	3190585	G
<i>In(3L)P</i>	3L	3191474	G
<i>In(3L)P</i>	3L	3192621	A
<i>In(3L)P</i>	3L	3194000	T
<i>In(3L)P</i>	3L	3195095	A
<i>In(3L)P</i>	3L	3198656	T
<i>In(3L)P</i>	3L	3202276	G
<i>In(3L)P</i>	3L	3203140	T
<i>In(3L)P</i>	3L	3203449	G
<i>In(3L)P</i>	3L	3205464	C
<i>In(3L)P</i>	3L	3244232	A
<i>In(3L)P</i>	3L	3250267	C
<i>In(3L)P</i>	3L	3251643	G
<i>In(3L)P</i>	3L	3258888	A
<i>In(3L)P</i>	3L	3260348	A
<i>In(3L)P</i>	3L	3274254	C
<i>In(3L)P</i>	3L	3284533	A
<i>In(3L)P</i>	3L	3388479	G
<i>In(3L)P</i>	3L	3389696	A
<i>In(3L)P</i>	3L	3390222	G
<i>In(3L)P</i>	3L	3397051	A
<i>In(3L)P</i>	3L	3430131	G
<i>In(3L)P</i>	3L	3764444	T
<i>In(3L)P</i>	3L	5399565	T
<i>In(3L)P</i>	3L	15633845	G
<i>In(3L)P</i>	3L	15970961	G
<i>In(3L)P</i>	3L	16165187	A
<i>In(3L)P</i>	3L	16165189	T
<i>In(3L)P</i>	3L	16165230	C
<i>In(3L)P</i>	3L	16170296	C
<i>In(3L)P</i>	3L	16193541	A
<i>In(3L)P</i>	3L	16201506	G
<i>In(3L)P</i>	3L	16217175	A
<i>In(3L)P</i>	3L	16222536	G
<i>In(3L)P</i>	3L	16223154	C

<i>In(3L)P</i>	3L	16261646	T
<i>In(3L)P</i>	3L	16261672	A
<i>In(3L)P</i>	3L	16261695	T
<i>In(3L)P</i>	3L	16261726	T
<i>In(3L)P</i>	3L	16263247	C
<i>In(3L)P</i>	3L	16263588	T
<i>In(3L)P</i>	3L	16268717	T
<i>In(3L)P</i>	3L	16273480	G
<i>In(3L)P</i>	3L	16280796	G
<i>In(3L)P</i>	3L	16280798	A
<i>In(3L)P</i>	3L	16289482	C
<i>In(3L)P</i>	3L	16290594	G
<i>In(3L)P</i>	3L	16290972	T
<i>In(3L)P</i>	3L	16291332	G
<i>In(3L)P</i>	3L	16297916	A
<i>In(3L)P</i>	3L	16298085	A
<i>In(3L)P</i>	3L	16301520	A
<i>In(3L)P</i>	3L	16308563	C
<i>In(3L)P</i>	3L	16311425	C
<i>In(3L)P</i>	3L	16326362	T
<i>In(3L)P</i>	3L	16333526	A
<i>In(3L)P</i>	3L	16377449	A
<i>In(3L)P</i>	3L	16378572	T
<i>In(3L)P</i>	3L	16393822	C
<i>In(3L)P</i>	3L	16400709	G
<i>In(3R)C</i>	3R	13114726	T
<i>In(3R)C</i>	3R	16099151	G
<i>In(3R)C</i>	3R	16104479	A
<i>In(3R)C</i>	3R	16110028	T
<i>In(3R)C</i>	3R	16114832	G
<i>In(3R)C</i>	3R	16145902	G
<i>In(3R)C</i>	3R	16145903	T
<i>In(3R)C</i>	3R	16191928	T
<i>In(3R)C</i>	3R	16864615	C
<i>In(3R)C</i>	3R	16893226	C
<i>In(3R)C</i>	3R	16918188	T
<i>In(3R)C</i>	3R	19748559	A
<i>In(3R)C</i>	3R	19755935	T
<i>In(3R)C</i>	3R	20442534	G
<i>In(3R)C</i>	3R	20498606	G
<i>In(3R)C</i>	3R	20558459	G
<i>In(3R)C</i>	3R	20924283	T
<i>In(3R)C</i>	3R	20943910	T
<i>In(3R)C</i>	3R	23033890	A
<i>In(3R)C</i>	3R	24007045	T
<i>In(3R)C</i>	3R	24007371	G

<i>In(3R)C</i>	3R	24009461	T
<i>In(3R)C</i>	3R	24014066	T
<i>In(3R)C</i>	3R	24029634	T
<i>In(3R)C</i>	3R	24041884	A
<i>In(3R)C</i>	3R	24041990	T
<i>In(3R)C</i>	3R	24043681	C
<i>In(3R)C</i>	3R	24044393	A
<i>In(3R)C</i>	3R	24078020	G
<i>In(3R)C</i>	3R	24085873	T
<i>In(3R)C</i>	3R	24096291	T
<i>In(3R)C</i>	3R	24138943	G
<i>In(3R)C</i>	3R	24142235	C
<i>In(3R)C</i>	3R	24150589	T
<i>In(3R)C</i>	3R	24163991	T
<i>In(3R)C</i>	3R	24171563	A
<i>In(3R)C</i>	3R	24172382	A
<i>In(3R)C</i>	3R	24195591	G
<i>In(3R)C</i>	3R	24201208	T
<i>In(3R)C</i>	3R	24242753	A
<i>In(3R)C</i>	3R	24243280	C
<i>In(3R)C</i>	3R	24279617	G
<i>In(3R)C</i>	3R	24282605	T
<i>In(3R)C</i>	3R	24298461	A
<i>In(3R)C</i>	3R	24342811	T
<i>In(3R)C</i>	3R	24374212	G
<i>In(3R)C</i>	3R	24409151	A
<i>In(3R)C</i>	3R	24422474	C
<i>In(3R)C</i>	3R	24467871	T
<i>In(3R)C</i>	3R	24487712	G
<i>In(3R)C</i>	3R	24493367	G
<i>In(3R)C</i>	3R	24506558	G
<i>In(3R)C</i>	3R	24512937	T
<i>In(3R)C</i>	3R	24522397	G
<i>In(3R)C</i>	3R	24551095	A
<i>In(3R)C</i>	3R	24690673	T
<i>In(3R)C</i>	3R	24693933	A
<i>In(3R)C</i>	3R	24694365	A
<i>In(3R)C</i>	3R	24719313	A
<i>In(3R)C</i>	3R	25096252	A
<i>In(3R)C</i>	3R	25106453	C
<i>In(3R)C</i>	3R	25136719	A
<i>In(3R)C</i>	3R	25175337	A
<i>In(3R)C</i>	3R	25176234	G
<i>In(3R)C</i>	3R	25179516	G
<i>In(3R)C</i>	3R	25193278	A
<i>In(3R)C</i>	3R	25216865	A

<i>In(3R)C</i>	3R	25222529	G
<i>In(3R)C</i>	3R	25242597	G
<i>In(3R)C</i>	3R	25248195	T
<i>In(3R)C</i>	3R	25269879	A
<i>In(3R)C</i>	3R	25315158	A
<i>In(3R)C</i>	3R	25329587	C
<i>In(3R)C</i>	3R	25474612	T
<i>In(3R)C</i>	3R	25489586	C
<i>In(3R)C</i>	3R	25505585	C
<i>In(3R)C</i>	3R	25538313	A
<i>In(3R)C</i>	3R	25560925	A
<i>In(3R)C</i>	3R	25567683	C
<i>In(3R)C</i>	3R	25583469	A
<i>In(3R)C</i>	3R	25596484	T
<i>In(3R)C</i>	3R	25598648	C
<i>In(3R)C</i>	3R	25599170	T
<i>In(3R)C</i>	3R	25604540	T
<i>In(3R)C</i>	3R	25604725	C
<i>In(3R)C</i>	3R	25605392	G
<i>In(3R)C</i>	3R	25605428	T
<i>In(3R)C</i>	3R	25632833	A
<i>In(3R)C</i>	3R	25647947	C
<i>In(3R)C</i>	3R	25680387	G
<i>In(3R)C</i>	3R	25686401	C
<i>In(3R)C</i>	3R	25686744	A
<i>In(3R)C</i>	3R	25689415	G
<i>In(3R)C</i>	3R	25689478	T
<i>In(3R)C</i>	3R	25692175	T
<i>In(3R)C</i>	3R	25776627	C
<i>In(3R)C</i>	3R	25789208	A
<i>In(3R)C</i>	3R	25789641	C
<i>In(3R)C</i>	3R	25798811	A
<i>In(3R)C</i>	3R	25810959	T
<i>In(3R)C</i>	3R	25822138	T
<i>In(3R)C</i>	3R	25830799	T
<i>In(3R)C</i>	3R	25836339	T
<i>In(3R)C</i>	3R	25865969	A
<i>In(3R)C</i>	3R	25881149	A
<i>In(3R)C</i>	3R	25884722	G
<i>In(3R)C</i>	3R	25885398	A
<i>In(3R)C</i>	3R	25885568	A
<i>In(3R)C</i>	3R	25892882	T
<i>In(3R)C</i>	3R	25893312	T
<i>In(3R)C</i>	3R	25901563	T
<i>In(3R)C</i>	3R	25904049	C
<i>In(3R)C</i>	3R	25904085	G

<i>In(3R)C</i>	3R	26052763	T
<i>In(3R)C</i>	3R	26450277	C
<i>In(3R)C</i>	3R	26502830	A
<i>In(3R)C</i>	3R	26541828	C
<i>In(3R)C</i>	3R	26553123	T
<i>In(3R)C</i>	3R	26833261	T
<i>In(3R)C</i>	3R	27033799	A
<i>In(3R)C</i>	3R	27050399	C
<i>In(3R)C</i>	3R	27050401	G
<i>In(3R)C</i>	3R	27183127	A
<i>In(3R)C</i>	3R	27187114	G
<i>In(3R)C</i>	3R	27189512	G
<i>In(3R)C</i>	3R	27213181	T
<i>In(3R)C</i>	3R	27230179	G
<i>In(3R)C</i>	3R	27255032	G
<i>In(3R)C</i>	3R	27348805	A
<i>In(3R)C</i>	3R	27350380	T
<i>In(3R)C</i>	3R	27355100	A
<i>In(3R)C</i>	3R	27355101	T
<i>In(3R)C</i>	3R	27367655	T
<i>In(3R)C</i>	3R	27376219	A
<i>In(3R)C</i>	3R	27450892	T
<i>In(3R)C</i>	3R	27536048	G
<i>In(3R)C</i>	3R	27560508	G
<i>In(3R)C</i>	3R	27560856	A
<i>In(3R)C</i>	3R	27561118	A
<i>In(3R)C</i>	3R	27813043	T
<i>In(3R)C</i>	3R	27815314	C
<i>In(3R)C</i>	3R	27819657	C
<i>In(3R)C</i>	3R	27873302	A
<i>In(3R)C</i>	3R	27885889	A
<i>In(3R)K</i>	3R	7569591	G
<i>In(3R)K</i>	3R	7587158	A
<i>In(3R)K</i>	3R	7763547	T
<i>In(3R)K</i>	3R	21961212	C
<i>In(3R)Mo</i>	3R	15955370	C
<i>In(3R)Mo</i>	3R	15956205	G
<i>In(3R)Mo</i>	3R	16012652	A
<i>In(3R)Mo</i>	3R	16054389	T
<i>In(3R)Mo</i>	3R	16088352	T
<i>In(3R)Mo</i>	3R	16101901	A
<i>In(3R)Mo</i>	3R	16309968	A
<i>In(3R)Mo</i>	3R	16310458	T
<i>In(3R)Mo</i>	3R	16321720	G
<i>In(3R)Mo</i>	3R	16324886	T
<i>In(3R)Mo</i>	3R	16327977	A

<i>In(3R)Mo</i>	3R	16329725	C
<i>In(3R)Mo</i>	3R	16354768	T
<i>In(3R)Mo</i>	3R	16358463	A
<i>In(3R)Mo</i>	3R	16477118	A
<i>In(3R)Mo</i>	3R	16505890	C
<i>In(3R)Mo</i>	3R	16563347	C
<i>In(3R)Mo</i>	3R	16564891	A
<i>In(3R)Mo</i>	3R	16565899	T
<i>In(3R)Mo</i>	3R	16825891	A
<i>In(3R)Mo</i>	3R	16840241	T
<i>In(3R)Mo</i>	3R	16877262	C
<i>In(3R)Mo</i>	3R	16881477	A
<i>In(3R)Mo</i>	3R	16882614	C
<i>In(3R)Mo</i>	3R	16914806	G
<i>In(3R)Mo</i>	3R	17081985	T
<i>In(3R)Mo</i>	3R	17145087	G
<i>In(3R)Mo</i>	3R	17161903	T
<i>In(3R)Mo</i>	3R	17183342	T
<i>In(3R)Mo</i>	3R	17190382	C
<i>In(3R)Mo</i>	3R	17203074	T
<i>In(3R)Mo</i>	3R	17226102	G
<i>In(3R)Mo</i>	3R	17231109	T
<i>In(3R)Mo</i>	3R	17252528	A
<i>In(3R)Mo</i>	3R	17255885	A
<i>In(3R)Mo</i>	3R	17257625	A
<i>In(3R)Mo</i>	3R	17261973	C
<i>In(3R)Mo</i>	3R	17346744	A
<i>In(3R)Mo</i>	3R	17482849	T
<i>In(3R)Mo</i>	3R	17492333	T
<i>In(3R)Mo</i>	3R	17512751	T
<i>In(3R)Mo</i>	3R	17543357	A
<i>In(3R)Mo</i>	3R	17570809	A
<i>In(3R)Mo</i>	3R	17574820	T
<i>In(3R)Mo</i>	3R	17575776	T
<i>In(3R)Mo</i>	3R	17614569	T
<i>In(3R)Mo</i>	3R	17618094	T
<i>In(3R)Mo</i>	3R	17653963	A
<i>In(3R)Mo</i>	3R	17673637	T
<i>In(3R)Mo</i>	3R	17731781	T
<i>In(3R)Mo</i>	3R	17752308	T
<i>In(3R)Mo</i>	3R	17775264	A
<i>In(3R)Mo</i>	3R	17798722	T
<i>In(3R)Mo</i>	3R	17812150	A
<i>In(3R)Mo</i>	3R	17812763	A
<i>In(3R)Mo</i>	3R	17833454	T
<i>In(3R)Mo</i>	3R	17871386	A

<i>In(3R)Mo</i>	3R	17878212	T
<i>In(3R)Mo</i>	3R	17893124	G
<i>In(3R)Mo</i>	3R	17900659	A
<i>In(3R)Mo</i>	3R	17905561	T
<i>In(3R)Mo</i>	3R	17909484	G
<i>In(3R)Mo</i>	3R	17914642	A
<i>In(3R)Mo</i>	3R	17915717	C
<i>In(3R)Mo</i>	3R	18018705	C
<i>In(3R)Mo</i>	3R	18110219	T
<i>In(3R)Mo</i>	3R	18151777	T
<i>In(3R)Mo</i>	3R	18195302	T
<i>In(3R)Mo</i>	3R	18227258	T
<i>In(3R)Mo</i>	3R	18229705	C
<i>In(3R)Mo</i>	3R	18236474	C
<i>In(3R)Mo</i>	3R	18237459	A
<i>In(3R)Mo</i>	3R	18248909	G
<i>In(3R)Mo</i>	3R	18405781	T
<i>In(3R)Mo</i>	3R	18747568	T
<i>In(3R)Mo</i>	3R	18755175	G
<i>In(3R)Mo</i>	3R	19051282	T
<i>In(3R)Mo</i>	3R	19310873	A
<i>In(3R)Mo</i>	3R	19540597	C
<i>In(3R)Mo</i>	3R	19573177	T
<i>In(3R)Mo</i>	3R	19604547	T
<i>In(3R)Mo</i>	3R	19614762	A
<i>In(3R)Mo</i>	3R	19616872	T
<i>In(3R)Mo</i>	3R	19619722	G
<i>In(3R)Mo</i>	3R	19621728	A
<i>In(3R)Mo</i>	3R	19625953	T
<i>In(3R)Mo</i>	3R	19686653	A
<i>In(3R)Mo</i>	3R	19690483	T
<i>In(3R)Mo</i>	3R	19928635	C
<i>In(3R)Mo</i>	3R	20090826	G
<i>In(3R)Mo</i>	3R	20102331	G
<i>In(3R)Mo</i>	3R	20106419	T
<i>In(3R)Mo</i>	3R	20108509	G
<i>In(3R)Mo</i>	3R	20712447	A
<i>In(3R)Mo</i>	3R	20717876	G
<i>In(3R)Mo</i>	3R	20720722	C
<i>In(3R)Mo</i>	3R	20761490	T
<i>In(3R)Mo</i>	3R	20809103	T
<i>In(3R)Mo</i>	3R	20815949	C
<i>In(3R)Mo</i>	3R	20837056	A
<i>In(3R)Mo</i>	3R	21380190	A
<i>In(3R)Mo</i>	3R	21807559	A
<i>In(3R)Mo</i>	3R	21956164	G

<i>In(3R)Mo</i>	3R	22035252	T
<i>In(3R)Mo</i>	3R	22399475	A
<i>In(3R)Mo</i>	3R	22436302	C
<i>In(3R)Mo</i>	3R	22477725	G
<i>In(3R)Mo</i>	3R	22635953	T
<i>In(3R)Mo</i>	3R	22660660	T
<i>In(3R)Mo</i>	3R	22661217	A
<i>In(3R)Mo</i>	3R	22703601	C
<i>In(3R)Mo</i>	3R	22850222	A
<i>In(3R)Mo</i>	3R	23028130	G
<i>In(3R)Mo</i>	3R	23504771	A
<i>In(3R)Mo</i>	3R	23589504	C
<i>In(3R)Mo</i>	3R	24757430	T
<i>In(3R)Mo</i>	3R	24834927	A
<i>In(3R)Mo</i>	3R	25052744	T
<i>In(3R)Mo</i>	3R	25065632	T
<i>In(3R)Mo</i>	3R	25087248	G
<i>In(3R)Mo</i>	3R	25206657	T
<i>In(3R)Mo</i>	3R	25250616	A
<i>In(3R)Mo</i>	3R	25253902	A
<i>In(3R)Mo</i>	3R	25293082	T
<i>In(3R)Mo</i>	3R	25354278	T
<i>In(3R)Mo</i>	3R	25687897	G
<i>In(3R)Mo</i>	3R	26584256	T
<i>In(3R)Mo</i>	3R	26725477	A
<i>In(3R)Mo</i>	3R	26930971	C
<i>In(3R)Mo</i>	3R	26933596	C
<i>In(3R)Mo</i>	3R	26949382	A
<i>In(3R)Mo</i>	3R	26955397	C
<i>In(3R)Mo</i>	3R	26960620	T
<i>In(3R)Mo</i>	3R	27080067	G
<i>In(3R)Mo</i>	3R	27091763	A
<i>In(3R)Mo</i>	3R	27114289	A
<i>In(3R)Mo</i>	3R	27124527	T
<i>In(3R)Mo</i>	3R	27136784	C
<i>In(3R)Mo</i>	3R	27266479	A
<i>In(3R)Mo</i>	3R	27382123	C
<i>In(3R)Mo</i>	3R	27395403	C
<i>In(3R)Mo</i>	3R	27395667	A
<i>In(3R)Mo</i>	3R	27396540	T
<i>In(3R)Mo</i>	3R	27396541	T
<i>In(3R)Mo</i>	3R	27419936	A
<i>In(3R)Mo</i>	3R	27430813	G
<i>In(3R)Mo</i>	3R	27434102	T
<i>In(3R)Mo</i>	3R	27434183	G
<i>In(3R)Mo</i>	3R	27434363	C

<i>In(3R)Mo</i>	3R	27438021	T
<i>In(3R)Payne</i>	3R	12257883	G
<i>In(3R)Payne</i>	3R	12259133	C
<i>In(3R)Payne</i>	3R	12259894	A
<i>In(3R)Payne</i>	3R	12263816	C
<i>In(3R)Payne</i>	3R	12289495	C
<i>In(3R)Payne</i>	3R	12298324	A
<i>In(3R)Payne</i>	3R	12298456	T
<i>In(3R)Payne</i>	3R	12316508	C
<i>In(3R)Payne</i>	3R	17442150	T
<i>In(3R)Payne</i>	3R	20343494	A
<i>In(3R)Payne</i>	3R	20562004	T
<i>In(3R)Payne</i>	3R	20567442	G
<i>In(3R)Payne</i>	3R	20567659	C
<i>In(3R)Payne</i>	3R	20567832	C
<i>In(3R)Payne</i>	3R	20575824	G
<i>In(3R)Payne</i>	3R	20580991	A
<i>In(3R)Payne</i>	3R	20580995	T
<i>In(3R)Payne</i>	3R	20590675	G
<i>In(3R)Payne</i>	3R	20591144	A

270 **Supporting Table 4. Inversion frequencies during the experimental evolution experiment.** Inversion frequencies estimated from Pool-Seq
 271 data using inversion-specific SNP markers in our laboratory natural selection experiment. Shown are median and average (in parentheses) of
 272 allele frequencies for each population.

Generation	Treatment	Replicate	<i>In(2L)t</i>	<i>In(2R)Ns</i>	<i>In(3L)P</i>	<i>In(3R)C</i>	<i>In(3R)K</i>	<i>In(3R)Mo</i>	<i>In(3R)P</i>
0	hot	1	0.39 (0.43)	0.1 (0.11)	0.16 (0.12)	0.16 (0.17)	0.01 (0.01)	0.04 (0)	0.21 (0.21)
0	hot	2	0.39 (0.31)	0.09 (0.1)	0.15 (0.25)	0.15 (0.16)	0.03 (0.06)	0.05 (0.08)	0.19 (0.18)
0	hot	3	0.43 (0.45)	0.09 (0.08)	0.14 (0.13)	0.15 (0.09)	0.01 (0)	0.05 (0.04)	0.19 (0.17)
15	hot	1	0.51 (0.56)	0.05 (0.06)	0.12 (0.07)	0.38 (0.57)	0.02 (0)	0.08 (0.07)	0.06 (0.18)
37	hot	1	0.39 (0.44)	0.02 (0)	0.13 (0.2)	0.41 (0.34)	0 (0)	0.06 (0.06)	0.02 (0.02)
59	hot	1	0.25 (0.34)	0 (0)	0.05 (0.04)	0.48 (0.5)	0 (0)	0.05 (0.05)	0 (0.04)
15	hot	2	0.43 (0.44)	0.03 (0.03)	0.25 (0.19)	0.36 (0.25)	0 (0)	0.04 (0)	0.07 (0.02)
37	hot	2	0.25 (0.12)	0 (0)	0.12 (0.31)	0.36 (0.27)	0 (0)	0.03 (0)	0.02 (0)
59	hot	2	0.25 (0.28)	0 (0)	0.03 (0)	0.27 (0.24)	0 (0)	0.07 (0.05)	0.01 (0.01)
15	hot	3	0.52 (0.5)	0.06 (0.04)	0.22 (0.22)	0.29 (0.34)	0 (0)	0.17 (0.11)	0.02 (0.01)
27	hot	3	0.32 (0.22)	0.04 (0.03)	0.16 (0.09)	0.37 (0.16)	0 (0)	0.12 (0.11)	0.02 (0.06)
37	hot	3	0.37 (0.37)	0.03 (0.02)	0.01 (0.05)	0.39 (0.3)	0 (0)	0.1 (0.1)	0.01 (0.09)
59	hot	3	0.23 (0.21)	0 (0)	0 (0)	0.5 (0.61)	0 (0)	0.01 (0)	0 (0.02)
15	cold	1	0.21 (0.21)	0.01 (0.01)	0.11 (0.08)	0.05 (0.08)	0 (0)	0.21 (0.16)	0.19 (0.22)
33	cold	1	0.39 (0.39)	0 (0)	0.07 (0.07)	0.07 (0.07)	0 (0)	0.22 (0.13)	0.03 (0.03)
15	cold	2	0.42 (0.42)	0.06 (0.02)	0.12 (0.2)	0.08 (0.06)	0 (0)	0.2 (0.18)	0.07 (0.07)
33	cold	2	0.21 (0.14)	0.01 (0.03)	0.11 (0.12)	0.16 (0.09)	0 (0)	0.24 (0.24)	0 (0)
15	cold	3	0.39 (0.39)	0.09 (0.09)	0.05 (0.11)	0.11 (0.03)	0 (0)	0.23 (0.28)	0.06 (0.04)
33	cold	3	0.56 (0.52)	0.02 (0)	0.07 (0.04)	0.15 (0.15)	0 (0)	0.28 (0.35)	0 (0)

273 **Supporting Table 5. Inversion frequency differences during experimental**
 274 **evolution.** *P*-values from CMH tests performed between the base population and
 275 consecutive generations during the experimental evolution experiment. *P*-values were
 276 combined by averaging across all marker SNPs for each inversion.

Inversion	0_15_hot	0_37_hot	0_59_hot	0_15_cold	0_33_cold
<i>In(2L)t</i>	0.3259	0.4464	0.0739	0.3081	0.5377
<i>In(2R)NS</i>	0.3757	0.1298	0.0139	0.3150	0.0209
<i>In(3L)P</i>	0.4246	0.2829	0.0032	0.3877	0.2022
<i>In(3R)C</i>	0.0275	0.0129	0.0012	0.2040	0.3445
<i>In(3R)K</i>	0.4080	0.4394	0.2045	0.4543	0.1755
<i>In(3R)Mo</i>	0.2035	0.4997	0.4699	0.0232	0.0071
<i>In(3R)Payne</i>	0.0048	0.0132	0.0009	0.0639	0.0000

277 **Supporting Table 6. Inversion frequencies in natural populations.** Inversion frequencies estimated from Pool-Seq data using inversion-
 278 specific SNP markers for the Australian (Kolaczkowski *et al.* 2011) and North American (Fabian *et al.* 2012) data. Median and average (in
 279 parentheses) of allele frequencies for each population.

	<i>In(2L)t</i>	<i>In(2R)Ns</i>	<i>In(3L)P</i>	<i>In(3R)C</i>	<i>In(3R)K</i>	<i>In(3R)Mo</i>	<i>In(3R)Payne</i>
Florida	0.41 (0.38)	0.01 (0.01)	0.09 (0.09)	0.01 (0)	0 (0)	0 (0)	0.49 (0.54)
Pennsylvania	0.23 (0.22)	0.04 (0.05)	0.01 (0.05)	0.01 (0)	0 (0.01)	0.08 (0.05)	0.02 (0.06)
Maine	0.2 (0.21)	0.1 (0.11)	0 (0.04)	0.02 (0.02)	0.06 (0.07)	0.14 (0.14)	0.01 (0)
Queensland	0.2 (0.38)	0.05 (0.04)	0.09 (0.08)	0 (0)	0 (0)	0 (0)	0.23 (0.13)
Tasmania	0 (0)	0 (0)	0 (0)	0 (0)	0 (0)	0 (0)	0.05 (0)

281 **Supporting Table 7. Inversion frequency differences in natural populations.**

282 *P*-values from Fisher Exact Tests (FET) performed between the lowest-latitude
 283 population (Florida and Queensland, respectively) and all other populations in North
 284 America (Florida-Pennsylvania: FP; Florida-Maine: FM) and Australia (Queensland-
 285 Tasmania: QT) (also see Kolaczkowski *et al.* 2011; Fabian *et al.* 2012). *P*-values were
 286 combined by averaging across all marker SNPs for each inversion.

287

Inversion	FP	FM	QT
<i>In(2L)t</i>	0.1848	0.0220	0.4987
<i>In(2R)Ns</i>	0.2692	0.0703	0.6332
<i>In(3L)P</i>	0.1172	0.0752	0.5460
<i>In(3R)C</i>	0.2043	0.3590	0.6584
<i>In(3R)K</i>	0.2500	0.1091	1.0000
<i>In(3R)Mo</i>	0.0853	0.0089	0.7476
<i>In(3R)Payne</i>	0.0000	0.0000	0.3516

288

289 **Supporting Table 8. Expected inversion frequency changes due to neutral**
 290 **evolution.** Here, we performed 100,000 simulations of inversion frequency changes
 291 as expected due to genetic drift based on a Wright-Fisher model and tested whether
 292 the changes were in the expected direction (sign of frequency change) and stronger
 293 than observed in the real data. The empirical *P*-value corresponds to the proportion of
 294 simulations resulting in stronger inversion frequency changes consistent across all
 295 replicates than observed in the real data from the laboratory natural selection
 296 experiment. Note that the frequency increases of *In(3R)C* in the hot and *In(3R)Mo* in
 297 the cold temperature treatment were significantly higher than expected due to genetic
 298 drift (*P*-value < 0.0042; Bonferroni corrected α of 0.05). Additionally, the frequency
 299 of *In(3R)P* significantly decreased stronger than expected due to neutral evolution in
 300 the cold temperature treatment. All significant results are indicated by an asterisk.

Inversion	Treatment	Generations simulated	Sign of frequency change	Empirical <i>P</i>-value
<i>In(2L)t</i>	cold	33	-	0.2105
<i>In(2L)t</i>	hot	59	-	0.0302
<i>In(2R)NS</i>	cold	33	-	0.0577
<i>In(2R)NS</i>	hot	59	-	0.1352
<i>In(3L)P</i>	cold	33	-	0.0994
<i>In(3L)P</i>	hot	59	-	0.0821
<i>In(3R)C</i>	cold	33	-	0.2033
<i>In(3R)C</i>	hot	59	+	0.0031*
<i>In(3R)Mo</i>	cold	33	+	0.0002*
<i>In(3R)Mo</i>	hot	59	-	0.5250
<i>In(3R)P</i>	cold	33	-	0.0020*
<i>In(3R)P</i>	hot	59	-	0.0152

301

302

299 **Supporting Table 9. Reliability of inversion frequency estimates.** *P*-values of FET tests used to test for significant differences between
 300 empirically determined inversion frequencies (via karyotyping) and those estimated from inversion-specific SNP markers. *P*-values were. Note
 301 that non of the *P*-values were significant, indicating that the two methods for estimating inversion frequencies did not differ from each other in
 302 their reliability.

303

Generation	Regime	Rep	<i>In(2L)t</i>	<i>In(2R)Ns</i>	<i>In(3L)P</i>	<i>In(3R)C</i>	<i>In(3R)K</i>	<i>In(3R)Mo</i>	<i>In(3R)P</i>
59	hot	1	0.29	1.00	1.00	1.00	1.00	1.00	1.00
59	hot	2	0.82	1.00	0.34	0.42	1.00	0.66	0.12
59	hot	3	0.08	1.00	1.00	0.44	1.00	1.00	1.00
33	cold	1	1.00	1.00	0.72	1.00	1.00	1.00	0.14
33	cold	2	0.31	1.00	0.33	0.16	1.00	0.83	1.00
33	cold	3	0.26	0.17	0.34	0.76	1.00	0.48	1.00

309 **Supporting Table 10. Allele sharing among karyotypes.** Amount of allele sharing
 310 between individuals (numbers 96 and 100) carrying *In(3R)Mo* and individuals with
 311 other chromosomal arrangements. We only used SNPs which were polymorphic
 312 between individuals 96 and 100 and the other *In(3R)Mo* chromosomes, located in two
 313 polymorphic regions within the inversion boundaries; region 1 spanned positions
 314 17,300,000 to 19,400,000 and region 2 positions 23,400,000 to 24,200,000.
 315

Chrom. region	Individual	No. of SNPs	<i>In(3R)C</i>	<i>In(3R)Payne</i>	Standard
1	96	382	63.97%	47.00%	100.00%
1	100	1197	73.77%	48.12%	78.11%
2	96	374	64.97%	56.15%	100.00%

316 **Supporting Table 11. Statistical power of inversion-specific marker alleles in**
 317 **terms of estimating inversion frequencies.** Exact P -values obtained by sampling
 318 from a χ^2 -distribution calculated from randomly drawn SNPs by means of CMH tests.
 319 Significant P -values ($P < 0.05$) indicate that inversion-specific markers performed
 320 better than SNPs randomly drawn from within the inversion body.

Inversion	0_15_hot	0_37_hot	0_59_hot	0_15_cold	0_33_cold
<i>In(2L)t</i>	0.2628	0.9400	0.0730	0.6709	0.9997
<i>In(2R)NS</i>	0.6501	0.0812	0.0000	0.8527	0.0000
<i>In(3L)P</i>	0.9989	0.9881	0.0003	0.5320	0.2976
<i>In(3R)C</i>	0.0000	0.0000	0.0000	0.0802	1.0000
<i>In(3R)K</i>	0.9727	0.9775	0.9711	0.9039	0.8684
<i>In(3R)Mo</i>	0.6842	1.0000	1.0000	0.0000	0.0000
<i>In(3R)Payne</i>	0.0000	0.0001	0.0000	0.0089	0.0000